

CrossMark  
click for updatesCite this: *RSC Adv.*, 2015, 5, 42109

# Conducting polymers and their inorganic composites for advanced Li-ion batteries: a review

Prakash Sengodu<sup>\*a</sup> and Abhay D. Deshmukh<sup>b</sup>

Conducting polymers are promising materials for organic–inorganic hybrid composites in lithium-ion batteries due to their electrical conductivity and high coulombic efficiency and are able to be cycled hundreds or thousands of times with only slight degradation. Inorganic compounds generally possess good lithium storage properties but lack the conductivity and cyclability required for commercial application. Therefore, these problems need to be overcome before they can be used as effective electrodes. Over the past few years, conductive polymers in combination with inorganic compounds have attracted great interest as promising matrices for the construction of lithium-ion batteries. Because conducting polymers can interact synergistically with inorganic compounds, noteworthy improvements in electrode lifetime, rate capabilities, and voltage, as well as mechanical and thermal stability, have been achieved. This review covers recent advances in synthetic methods and functions of conducting polymers in hybrid composites and their application in lithium-ion batteries. We then present a comparison of other synthetic methods for new research and development in batteries. A brief appraisal of avenues for future developments in this area is also presented.

Received 30th December 2014  
Accepted 10th April 2015

DOI: 10.1039/c4ra17254j

www.rsc.org/advances

## 1. Introduction

The urgent need for clean and secure energy has stimulated a global revival in the search for advanced electrical energy storage systems. The predicted future lithium ion batteries (LIBs) are one of the most promising sources of energy storage. So far, lithium metal electrodes have been troublesome due to their unsatisfactory cycling life, which results eventually in

<sup>a</sup>Department of Chemistry, National Taiwan Normal University, Taipei, Taiwan.  
E-mail: prakas.chemist@gmail.com

<sup>b</sup>Energy Materials and Devices Laboratory, Department of Physics, RTM Nagpur University, Nagpur, India. E-mail: abhay.d07@gmail.com



Prakash Sengodu did his M.Sc in Chemistry at Sri Ramakrishna Mission Vidyalaya, Tamil Nadu, India in 2006 and he completed his PhD at CSIR-Central Salt and Marine Chemicals Research Institute, Bhavnagar, India. He was awarded a Senior Research Fellowship and Research Internship from CSIR India. He has also worked as a Research Fellow at Central Electrochemical Research Institute,

India, on conducting polymers. In 2013, he was awarded a National Science Council (NSC) Postdoctoral Fellowship and worked in National Taiwan Normal University (NTNU), Taiwan with Prof. C. J. Chen. His research interests include conducting polymers for electrochemical applications. He may be reached at prakas.chemist@gmail.com.



Abhay D. Deshmukh obtained his M.Sc. and PhD in Physics from Nagpur University, and CSIR-National Environmental Engineering Research Institute, India. He has worked as a Research Associate at National Physical Laboratory, New Delhi, India. Then he was awarded a National Science Council (NSC) Postdoctoral Fellowship and worked in National Taiwan Normal University (NTNU), Tai-

wan with Prof. C. J. Chen. He is now working as an assistant professor in the Department of Physics, R.T.M. Nagpur University, India. His research interest is nanomaterials and their optical properties as well as advanced carbon materials and composites for batteries and supercapacitors. He may be reached at abhay.d07@gmail.com.

shorting between the two electrodes, less safety and low rate capability.<sup>1–3</sup> Commercial LIBs with LiCoO<sub>2</sub>, graphite and a non-aqueous Li salt as cathode, anode and electrolyte, respectively, based on an intercalation and deintercalation mechanism were developed by Sony Co., Japan in 1991. They are a good sign of solid-state chemistry in action, whose details may be found in the literature.<sup>4</sup> Fig. 1 shows promising present and future energy storage systems plotted by price vs. energy. From this plot, the energy density of a Li-ion battery is higher than that of a supercapacitor and a Na-ion battery due to its low-radius ions and numerous atoms, which are easy to insert into electrode materials. However, the energy density of a Li-ion battery is lower than that of the corresponding air and sulfur batteries. The price of a Li-ion battery is higher than that of supercapacitors, Na-ion batteries and Li-S/air batteries. Current LIBs are widely used in hybrid electric vehicles (HEVs), cellular phones, laptops, camcorders, power tools, and medical fields. Sales of LIBs have increased by 1.5 per cent annually to \$10.6 billion in 2012 and are expected to rapidly increase to a market value of US \$31.4 billion in 2015 and US \$53.7 billion in 2020, due to their use in hybrid electric vehicles (HEVs) and plug-in electric vehicles (PEVs).<sup>5</sup> However, cost and safety issues are the main problems with the use of LIBs in electrical vehicles and smart grids.<sup>5–7</sup> Recently developed high-energy-density systems (Li-S and Li-O<sub>2</sub> batteries) would be more suitable for electric vehicles. However, some issues are major concerns for Li-S and Li-O<sub>2</sub> batteries due to low levels of dissolution of the electrode materials, which results in capacity decay.<sup>5–7</sup> The high rate capability and high energy density of Li-ion supercapacitors make them good systems for replacing present lead-acid batteries for car starter batteries. Research into sodium ion batteries (NIBs) is a newly growing field compared to that into other battery types, due to their abundance and low price. Trona (sodium ore) is 30 times cheaper than lithium carbonate.<sup>6</sup> Many efforts are also being made to develop sodium batteries for electric vehicles and grid storage applications, which are the most promising in the near future.<sup>7</sup>

In recent years, the design and fabrication of electrodes has gained much attention in applications of rechargeable batteries. The subject of tuning electrodes has also remained an

important area of research activity. With respect to batteries, much emphasis has been placed on the fabrication and characterization of hybrid composites.<sup>8,9</sup> These are also of great research interest as emerging electrodes in academia and industry, due to their structural diversity, flexibility and durability as well as high porosity, and therefore a wide spectrum of applications in sensors, solar energy, batteries and supercapacitors have been investigated.<sup>10</sup> Interest in inorganic compounds is motivated by their potential applications in lithium-ion batteries,<sup>11</sup> due to their easy transport of Li<sup>+</sup> ions and electrons allowing better accommodation of ions. Inorganic materials also play diverse roles in different battery systems.<sup>12</sup> In general, their good crystallinity, excellent conductivity and redox properties make them suitable as “electrodes” (anodes and cathodes) and photocatalysts (due to their nanometer size and structure).<sup>13,14</sup>

Conducting polymers (CPs) are not just intended for use in energy storage but are also used to do so independently of their form. Their mechanical properties are like those of a plastic, allowing them to be twisted, contracted, and stiff.<sup>15–17</sup> CPs electrodes can be incorporated seamlessly into electronic paper, textiles, data tattoos, structural panels, *etc.*, without including traditional prismatic or cylindrical cells.<sup>17–19</sup> They are also used to directly combine the properties of a plastic with polymer solar cells and light-emitting diodes in a streamlined manufacturing process to produce cheap flexible devices.<sup>20,21</sup> Furthermore, they have many advantages of synthetic tailorability, cost, and processability, which make them ideal candidates for electrochemical energy storage.<sup>22,23</sup> Their properties may be changed by synthetic techniques.<sup>24</sup> Also, the raw materials and methods for making these polymers are often cost-effective. New synthetic methods have enhanced their processability *via* screen printing, doctor blading, or inkjet printing.<sup>25,26</sup>

Mainly, conducting polymers are ideal materials for hybrid composites in lithium-ion batteries due to their conducting backbone, electrical conductivity and high coulombic efficiency; thus, they can be cycled hundreds or thousands of times with little degradation.<sup>20,27–29</sup> Their conductive nature arises from alternating single and double carbon-carbon bonds in polymeric chains, which can be assigned to reversible chemical, electrochemical and physical properties controlled by a doping process. Inorganic materials exhibit high capacity based on a lithium insertion and extraction process but lack the conductivity and cyclability required for commercial application. Overcoming these problems, conducting polymers can interact synergistically with inorganic materials by a mixture of synthetic tuning, processing options, and mechanical flexibility, which can result in polymer power sources that can be designed to suit the device rather than *vice versa*.<sup>30–32</sup> Also, CPs can be used alone as anode/cathode electrodes due to their doping nature and exchange of anions. Therefore, high specific capacity can be achieved by concentrating the electrolyte; however, system batteries with high specific energies at mean cell voltages of up to 3.5 V are possible. CPs not only have advantages with their potential response in a state of charge or discharge, but also disadvantages such as the inclination in their characteristic discharge curve. Of particular note is

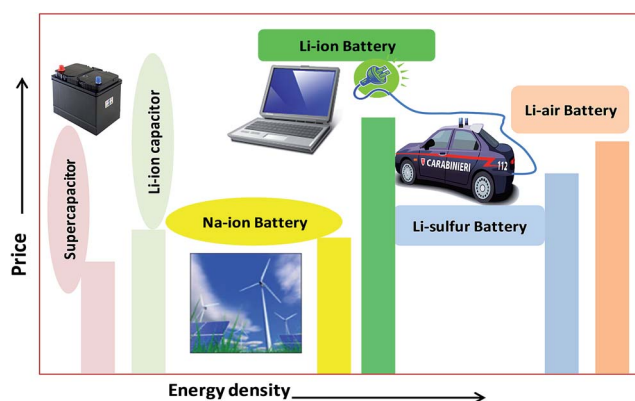


Fig. 1 Plot of price vs. energy density for different energy storage systems.

polyaniline, which was once a cathode in a PANI lithium battery commercially available from Bridgestone–Seiko in the 1980s. Table 1 presents a comparison between commercial electrodes and conducting polymers.<sup>33–41</sup>

Popular research into conducting polymer electrodes for lithium-ion batteries has only focused on polyaniline (PANI), polypyrrole, and polythiophene (PT) and their derivatives.<sup>42,43</sup> The focus has been on these particular polymers due to the presence of wide background research, the commercial accessibility of both monomers and polymers, and their simplicity of synthesis. Inorganic compounds display low capacity utilization, inferior rate capability, poor cycling stability, or even complete electrochemical inactivity in LIBs. Therefore, numerous articles have been devoted to polymers embedded with inorganic compounds in electrodes as an additive to improve the performance of cathode and anode materials in batteries. Earlier reviews have focused on Si/SiO<sub>2</sub>, Sn/SnO, TiO<sub>2</sub>, carbon, graphene, and intermetallic compounds as cathode/anode materials,<sup>44–46</sup> with some attention to binders.<sup>47</sup> To the best of our knowledge, there is still no review on conducting polymer–inorganic compound hybrid composite electrodes for battery applications. The fundamental electrochemical aspects of conducting polymers have been discussed in review papers and books covering the literature up to 1997.<sup>48</sup> The aim of the present review is to provide information on hybrid composite electrodes in the light of applications of rechargeable batteries in the past decades. Here, we discuss the preparative methods of rechargeable battery electrodes and issues affecting their electrochemical properties. These include low energy, low capacity and power density, oxidative stability, and diffusion limitations on dopant ions. Numerous recent advances in the field have made remarkable progress in addressing these issues and will be discussed in this review.

### 1.1. Mechanism of conducting polymers in rechargeable batteries

In brief, in rechargeable batteries inorganic ions (M<sup>+</sup>) are moved freely by the electrolyte from the anode to the cathode as electrons flow through an external circuit from the anode to the cathode, producing power during discharge. During recharge, M<sup>+</sup> and electrons are driven in the reverse direction by an external voltage, storing electrical energy as chemical energy in the battery (Fig. 2). Several parameters, including gravimetric

energy density (mW h g<sup>-1</sup>), gravimetric capacity (mA h g<sup>-1</sup>), volumetric capacity (mA h cm<sup>-3</sup>), rate capability, cycling ability and self-discharge characteristics, are influenced by the choice of battery materials and battery design. Anode materials function by three different mechanisms, an intercalation–deintercalation mechanism, alloying–dealloying reactions, and redox or “conversion” reactions, whereas cathode materials follow a two-phase mechanism of the classic shrinking core model, anisotropic shrinking core model, and domino-cascade model.<sup>48–50</sup>

During the charge/discharge process, anode materials undergo a large volume change (>300%), which causes great strain in the material and thus leads to cracking and crumbling of particles. It results in poor reversible capacity and irreversible capacity loss in the first cycle. For example, in Si-based electrodes during transformation from Si to Li<sub>4.4</sub>Si the volume expansion is about 420%. These electrodes are typically inferior in capacity retention. Early studies on Si anodes confirmed rapid capacity fade during cycling.<sup>51–54</sup> During cycling of silicon (average particle size 10 μm), high capacity is reached in the first lithiation, but after that capacity rapidly fades. Even the reversible capacity of a Si electrode drops by 70% after only five cycles. Moreover, the irreversible capacity loss of this Si anode during the first cycle is excessively high (2650 mA h g<sup>-1</sup>) for practical application, with a coulombic efficiency of 25%. The overall capacity loss and huge initial irreversible capacity loss with Si anodes are caused by large volume changes during the lithium insertion/extraction processes. The solution is a tailored polymer that conducts electricity and binds closely to Li/Na-storing particles with the advantages of low cost and compatibility. In addition, anodes expand to more than three times their volume during charging and then shrink again during discharge. Also, very few studies have claimed a polymer alone as an anode for batteries (usually single experimental cells with a few milligrams of polymer and excess electrolyte) based on a doped (oxidized or reduced) state.<sup>55</sup> Conducting polymers have also been cathodes satisfactorily combined with inorganic redox oxides, giving systems suitable for electrochemical Li intercalation with improved performance.<sup>48</sup> Polymers can decrease polarization between the cathode particles and the electrolyte and also promote permeation of the electrolyte into the surface of the active particles, hence enhancing M<sup>+</sup> insertion–extraction during the cycling process.<sup>56</sup> There have been many reports on the role of PANI in cathode materials, such as improving the

Table 1 Performance characteristics of conjugated polymers compared to current inorganic Li-ion battery materials

Electrode	Voltage vs. Li/Li <sup>+</sup>	Mw of repeating unit	Capacity (mA h g <sup>-1</sup> )		Energy density (mW h g <sup>-1</sup> )	Power density (mW h g <sup>-1</sup> )
			Theor.	Expt.		
Graphite <sup>33</sup>	~0.1	12	372	360	372–744	—
LiCoO <sub>2</sub> (ref. 34)	~3.8	97.9	274	135	30–144	100–1000
LiFePO <sub>4</sub> (ref. 35)	~3.2	157.8	170	109	90–100	23–70
Polythiophene <sup>36,37</sup>	3.1–4.0	82.1	326	82	93	89
Polypyrrole <sup>38,39</sup>	3.0–4.0	65.1	412	82	60	10
PEDOT <sup>40</sup>	2.7–4.2	140.2	191	30–70	1–4	35–2500
Polyaniline <sup>41</sup>	3.0–4.0	91.1	294	100–147	300	100

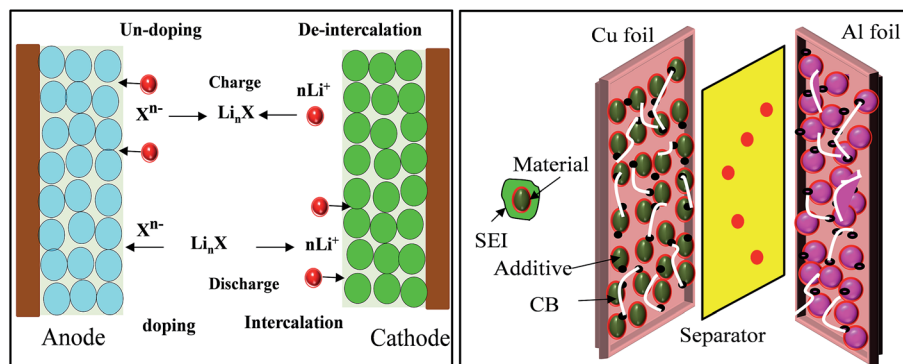


Fig. 2 Principle of LIBs based on doping/dedoping (negative) and deintercalation/intercalation (positive) electrodes and a model of the electrodes with their SEI system.

electrical conductivity, decreasing polarization, and promoting electrolyte permeation.<sup>56–58</sup> Conducting polymers alone are used as electrodes in LIBs applications, but their poor capacity limits their practical application.<sup>59,60</sup>

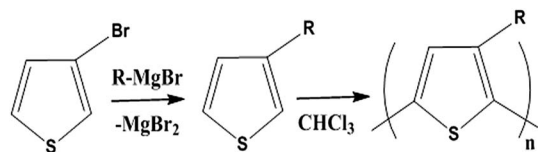
## 1.2. Synthetic methods of conducting polymers

Conductive polymers are organic polymers that conduct electricity and may exhibit metallic conductivity or can be

semiconductors. They are organic materials and similar to insulating polymers, but are not thermoplastics or thermoformable.<sup>15–17</sup> Table 2 shows the conductivity of different conductive polymers.<sup>61,62</sup> They offer high electrical conductivity but do not have comparable mechanical properties to other commercially available polymers. Their electrical properties can be fine-tuned using methods of organic synthesis and advanced dispersion techniques.<sup>63,64</sup> Heeger, MacDiarmid and Shirakawa were Nobel Laureates for their discovery of metallic

Table 2 List of some of the most important conducting polymers and their structure, conductivity and type/doping

Polymer	Conductivity ( $S\text{ cm}^{-1}$ )	Type/doping
Polyacetylene <sup>61</sup>	200–1000	n, p
Polyparaphenylene <sup>61</sup>	500	n, p
Polyparaphenylene sulfide <sup>61</sup>	3–300	p
Polythiophene <sup>61</sup>	10–100	p
Polypyrrole <sup>61</sup>	40–200	p
Polyisothianaphthalene <sup>61</sup>	1–50	p
Polyparaphenylene vinylene <sup>61</sup>	1–1000	p
Polyaniline <sup>62</sup>	1–100	p

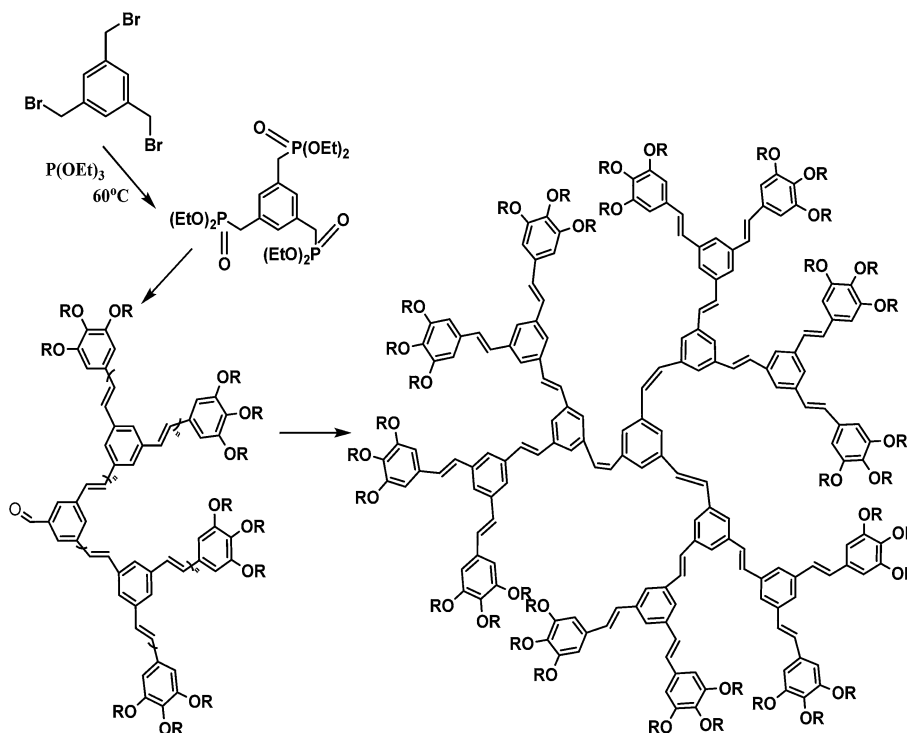


Scheme 1 The most common route to poly(3-alkylthiophenes).

conductivity in a polymer in polyacetylene (PA).<sup>65</sup> It has been clear that the great potential in the development of organic semiconductors was related to the ability of macromolecular chemists to synthesize new structures having a conjugated backbone. The main aims of synthetic procedures were to overcome the drawbacks of their insolubility and unprocessability.<sup>66</sup> Several synthetic methods have been developed in the past three decades. Some of these represented innovative strategies in macromolecular synthesis and were responsible for the evolution of chemistry in the polymer field. The Ziegler-Natta catalyst is foremost for chemical polymerization of acetylene among the various catalyst systems (radiation, cationic, transition/rare-earth metal, *etc.*) that can be used to initiate polymerization.<sup>67</sup>  $\text{Ti}(\text{OBu})_4/\text{AlEt}_3$  and  $\text{NaBH}_4/\text{Co}(\text{NO}_3)_2 \cdot 6\text{H}_2\text{O}$  catalysts have also been well studied.<sup>68,69</sup> Stable conducting polymers have been synthesized by physically blending conjugated polymers with certain non-conjugated macromolecules<sup>70</sup> and chemically synthesizing conducting polymer colloids<sup>71</sup> or conjugated oligomers.<sup>72</sup> Recent synthetic routes have now been devised for preparing stable conducting polymers, as described below.

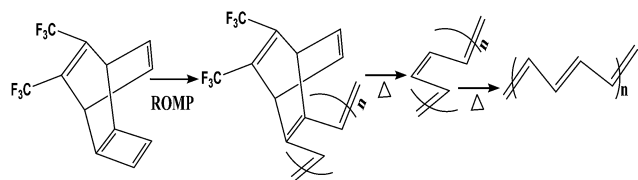
Soluble polymers have been synthesized by different methods such as substitution and copolymerization (random and alternating copolymerization, block and graft copolymerization). Generally, the chemical and physical properties of a polymer material can change with substitution; therefore, soluble forms of various conducting polymers have been prepared by grafting suitable side groups or side chains onto polymer backbones. Yoshino *et al.* reported polyacetylene grafted with methyl or phenyl side groups.<sup>73</sup> Tamao *et al.* prepared poly(3-alkylthiophenes), which were melttable and soluble in most common organic solvents, from 3-bromothiophene (Scheme 1).<sup>74</sup> Soluble polypyrrole and polyaniline have also been synthesized by introducing alkyl side groups,<sup>75</sup> and grafting with hydrophilic side groups/chains ( $-\text{SO}_3\text{H}$ ,  $-\text{COOH}$ ,  $-\text{OH}$ ) even allows the formation of water-soluble conducting polymers.<sup>76</sup> Copolymerization of conjugated polymers with various soluble sections provides an alternative way to overcome the uncontrollability of conjugated polymers. The combination of optoelectronic properties characteristic of conjugated structures and the solubility of soluble polymeric segments into a single copolymer chain should, in principle, lead to a material that exhibits properties of both constituent components. Meier *et al.* have synthesized some highly soluble stilbenoid dendrimers with alkoxy chains substituted on the peripheral benzene rings (Scheme 2).<sup>77</sup>

For the preparation of conjugated polymer films, they developed solution process techniques (spin coating), precursor routes and electropolymerisation methods. The solution process method offers excellent possibilities for the fabrication of advanced devices, but it may cause problems in the quality of



Scheme 2 Synthesis of highly soluble stilbenoid dendrimers with alkoxy chains substituted on the peripheral benzene rings.





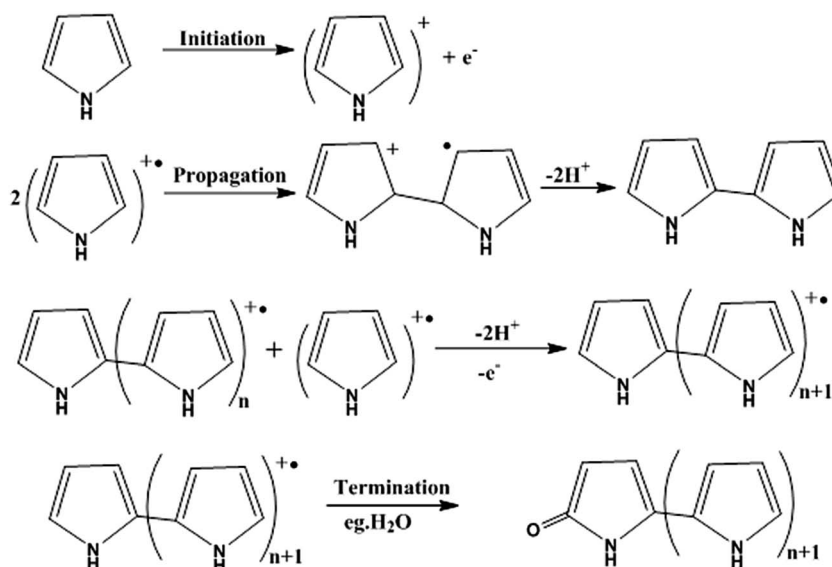
Scheme 3 Durham route to polyacetylene (PA). ROMP = ring-opening metathesis polymerization.

polymer films thus formed, such as possible deterioration in the mechanical properties of polymer films by chemical modification of their structures, reduction of the stability of devices by trapped impurities and complications in choosing a suitable solvent for preparing pinhole-free multi-layer polymer thin films. Thermal conversion of soluble non-conjugated precursor polymers has tried to overcome the uncontrollability of the formation of conjugated polymers. Edwards and Feast *et al.* reported the ring-opening metathesis polymerization (ROMP) of cyclobutene derivatives, followed by thermal conversion into polyacetylene with the evolution of bis(trifluoromethyl)benzene (Scheme 3). Both the potentiostatic method with a constant potential and the potentiodynamic technique by scanning the potential within a certain range of voltages have been used for electrochemical polymerization of electrically conducting polymers. Pyrrole can be polymerized on a suitable anode using a two-electrode electrochemical cell. The mechanism of the electropolymerization of pyrrole is suitable for many other conjugated conducting polymers (Scheme 4).<sup>78</sup>

In general, oxidation is used to provide the driving force for polymer synthesis, whether this is *via* the addition of a chemical oxidant (ammonium persulfate) or by the application of an oxidizing electrochemical potential to the surface of a submerged electrode.<sup>79</sup> As this process is carried out in an oxidizing environment, the ensuing polymers are formed in an

already doped state. For example, PANI is synthesized in the emeraldine salt form in oxidative conditions, whereas reductive polymerization produces polythiophene as an n-type polymer.

Recently, nanostructured conducting polymers have been synthesized by versatile methods which are suitable for their applications. Long *et al.* discussed the synthetic methods in detail.<sup>80</sup> The hard-template method provides aligned arrays of tubes and wires with controllable length and diameter, with the disadvantage that a post-synthetic process is needed to remove the template. For example,  $\text{MnO}_2$ /poly(3,4-ethylenedioxythiophene) (PEDOT) coaxial nanowires were synthesized by co-electrodeposition in a porous alumina template. The soft-template method is another powerful and popular technique for producing CPs, but it does not provide uniform morphology in samples, for example, PANI micro/nanostructures. By now, structure-directing molecules, surface micelles, surfactants, liquid crystal or colloidal particles or phases, and aniline oligomers used as soft templates, have been developed, as have rapidly mixed reactions, reverse emulsion polymerization, template-free methods, ultrasonic irradiation, interfacial polymerization, dilute polymerization, and radiolytic synthesis.<sup>81–89</sup> Kaner *et al.* proposed the interfacial polymerization method, which involves step polymerization of two monomers respectively dissolved in two immiscible phases; therefore, the reaction takes place at the interface between the two liquids. It is usually based on self-assembly mechanisms caused by hydrogen bonding, van der Waals forces, double-bond stacking, and electrostatic interactions as driving forces.<sup>81,82</sup> Wan proposed the template-free method as simple self-assembly without an external template. By controlling synthesis conditions, including temperature and the molar ratio of monomer to dopant, polyaniline and polypyrrole nanostructures can be synthesized by *in situ* doping polymerization in the presence of dopants. In the self-assembly formation mechanism the micelles formed by dopants and/or monomers act as soft



Scheme 4 Mechanism for the electropolymerization of pyrrole, which is also valid for many other conjugated conducting polymers.

templates in the process of forming tubes/wires.<sup>84</sup> Up to now, a variety of polyaniline micro/nanostructures have been established.

Electrospinning is an efficient approach for constructing lengthy polymer fibers with diameters from microns to the nanoscale using strong electrostatic forces<sup>90,91</sup> (Fig. 3). In the electrospinning process, a polymer solution is extruded from an orifice to form a small droplet in the electric field which is present, and jets of the charged solution are extruded from a cone. Usually, extension of the fluid occurs uniformly first, and then the straight lines of flow undergo a vigorous whipping or splitting motion due to fluid instability and electrically driven bending instability. Then, the spun fibers are set down in the form of a non-woven web on a collector. Using an improved or modified electrospinning device, nanofibers with partial or even good orientation could be fabricated.<sup>90,91</sup> For example, micro- and nanoscale fibers of polyaniline/polyethylene oxide (PEO) have been prepared.<sup>91</sup> Soft lithography is a low-cost approach for shaping an initially flat polymer film using a micro-mold at high temperature or in the presence of solvent vapours. Recently, Huang *et al.* proposed a technique based on nanoimprint lithography and a lift-off process for patterning CPs.<sup>92</sup> Directed by an electrochemical technique for nanowire assembly, CP wire is electrochemically polymerized and assembled onto two biased anode and cathode electrodes immersed in aqueous monomer solutions.<sup>93</sup> Nanolithography is used for the fabrication of luminescent nanostructures and conductive polymer nanowires of controlled size using a dip pen.<sup>94</sup> Recently, the whisker method has been used for the production of self-assembled conducting polymer nanofibers by anisotropic crystallization in a nematic liquid crystal and achieved large-scale alignment of nanofibers.<sup>95</sup>

### 1.3. Functions of conducting polymers

To realize the functions of conducting polymers within the structure of a battery electrode, firstly we have to assess the

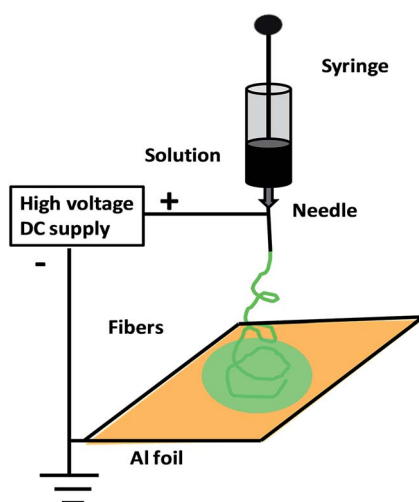


Fig. 3 Schematic of electrospinning method for the synthesis of conductive polymer nanofibers.

basic properties of conducting polymers themselves. Their conductivity and charge storage ability depend on electronic properties not possessed by the aliphatic group of polymers, which arise from the overlap of adjacent p-orbitals. The backbone of a conjugated polymer and its molecular orbitals provide a band structure similar to that observed in inorganic semiconductors.<sup>96</sup> The effective conjugation length is the point at which no extra monomer units added to the chain affect the electronic properties of the polymer.<sup>97</sup> The energy levels of the HOMO and LUMO conduction band of a polymer help determine its stability properties, its optical absorption wavelengths, and whether a polymer is more likely to be n-type or p-type.<sup>98</sup> The HOMO increases in energy and LUMO decreases in energy with increasing conjugation length. A polymer is more susceptible to electrophiles, *i.e.* more reactive, with a higher HOMO.

Polymers are classified as reduced (n-type) and oxidized (p-type) according to their dopant counterions. Due to their ability to stabilize positive charge, electron-rich polymers that have elevated HOMO levels comprise p-type materials. Due to their ability to stabilize negative charge, electron-poor polymers that have low-lying LUMO levels comprise n-type materials.<sup>99</sup> The p-doped polymers act as cathodes and there has been much work on them, but little focus on n-doped polymers acting as anodes.<sup>100</sup> Both electrodes must be used in flexible polymer batteries and therefore there is a need to research new n-type electrode materials as well. Polymers can be doped *via* either chemical or electrochemical processes.<sup>101</sup> A model of the doping process is presented in Fig. 4 for p-doping and n-doping. Doping generates radical cations or anions (positive/negative polarons), which are delocalized in the polymer backbone and provide a proposed mechanism of conductivity.<sup>102</sup> Charge delocalization is coupled with structural reorganization into a quinoidal form and a change in fundamental molecular vibrations.<sup>102</sup> UV/vis and IR/Raman spectra can be used to confirm the appearance of new sub-gap energy states and the formation of a quinoidal structure.<sup>102</sup> Generally, polymers in their native state have very low conductivities, of the order of  $10^{-4}$ – $10^{-9}$  S  $\text{cm}^{-1}$ , but can attain high conductivities when doped.<sup>103</sup> Redox reactions coupled with polymer doping coexist with the movement of ions into and out of the polymer matrix to provide charge neutrality.<sup>79</sup> Although oxidation generally results in movement of anions within the film, movement of cations occurs in certain conditions as well.<sup>104</sup> Movement can also occur for anions during polymer reduction. Growing dense polymer films tend to react more slowly due to ion transport limitations, which cause lower capacities and lower energy and power densities.<sup>105</sup> Nanostructured polymers such as nanowires, nanotubes, and nanoparticles can help alleviate trouble associated with ion diffusion by increasing the surface area and porosity.<sup>105</sup> By promoting oxidative stability, ion diffusion also influences electrode performance. The specific capacity of an electrode is determined by the number of monomer units over which charge is delocalized. This amounts to one unit of charge for every two to three monomer units, although higher levels of charge are likely for most polymers.<sup>79</sup> Higher levels of oxidation or reduction lead to a higher specific capacity in polymers, but high levels of charge can lead to deterioration of the polymer

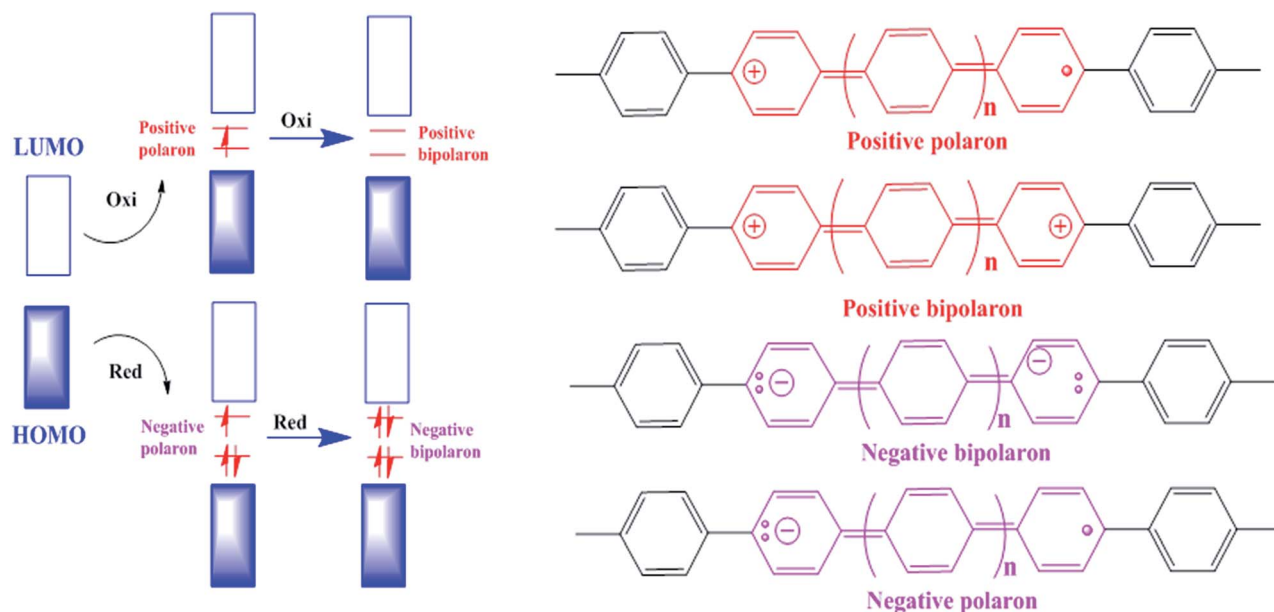


Fig. 4 Design of polyphenylene electronic and chemical structural changes during (a) oxidation (p-doping) and (b) reduction (n-doping). A radical cation (positive polaron) is formed *via* oxidation, while a radical anion (negative polaron) is formed during reduction. High states of charge can lead to the formation of positive and negative bipolarons. Cations and anions counterbalance charges in the polymer chain.

matrix *via* useless inter-chain interactions or the collapse of polymer chains.<sup>106</sup> Highly charged species are much more likely to react with common electrolytes and oxygen in the air as well.<sup>102</sup> Low capacities can be alleviated to a limited extent by the selection of dopant ion, electrolyte, or polymer structure.<sup>106</sup> There is evidence that strong interactions between highly charged or doped polymers and a complementary polyion can serve to stabilize well-oxidized polymers.<sup>107</sup> Deficiencies associated with stability over many charge cycles have seen enhancements *via* selected composite materials of carbon nanotubes or graphene.<sup>108</sup>

#### 1.4. Merits and demerits of conducting polymers

Most research interest in the conducting polymers, such as polyaniline (PANI), polypyrrole, and polythiophene (PT), continues to grow due to their oxidative stability, relatively high theoretical capacity, simple synthesis, and electrochemical reversibility.<sup>34</sup> PANI electrodes make use of reversible reactions between fully reduced and partially oxidized salt states. Their cycling stability can break down as the emeraldine salt is irreversibly oxidized to pernigraniline base, due to the reaction pathway to the pernigraniline salt not being favoured at higher potentials.<sup>109</sup> There have been some efforts to stabilize the pernigraniline salt and allow an increase in PANI's capacity along with its energy density.<sup>41</sup> However, although it has many merits, difficulties with the utilization of PANI stem from its insolubility, diffusion issues, cycling, and stability. Insolubility and uncontrollability are usually considered the main issues obstructing its usage in energy storage.<sup>110</sup> These problems had traditionally been addressed by dispersing the polymer in solutions using a series of steps intended to remove aggregates and ensure a stable suspension.<sup>111</sup> Polyanions with PANI

nanofibers using a template have allowed easy suspension in solution for PANI<sup>112</sup> and assembled with a carbon composite have helped maintain conductivity when PANI has been reduced to a non-conductive state, and so offer promising energy storage.<sup>110–112</sup> However, they can suffer from inferior capacity *vs.* redox-active materials due to the non-Faradaic nature of charge storage.<sup>113,114</sup> PANI nanostructures can also be produced economically and quickly in solution in the absence of templates, additives, or difficult techniques,<sup>115</sup> but they have uncontrollability issues because they are easily suspended in solution and stay so for extended periods of time.<sup>112</sup> PANI is a promising material for composites with high-capacity inorganic and carbon-based materials, which allows a facile solution. Our work has demonstrated good conductivity with even lower loadings of PANI/polyelectrolyte (poly-(diallyldimethylammonium chloride)), such as 4.5 to 42  $\mu\text{S cm}^{-1}$ .<sup>16</sup> Overall, investigation of PANI composites demonstrated significant effects on energy devices because the two components work together synergistically to improve coulombic efficiency and charge transport. There are methods for boosting charge capacity, without compromising the properties of a polymer, by including redox-active components in the polymer structure. Goodenough *et al.* reported developments in both the capacity and long-term cyclability of polypyrrole by covalently anchoring ferrocene groups to the polymer.<sup>116</sup> Ferrocene-functionalized triphenylamine polymer and 2,2,6,6-tetramethylpiperidine-*N*-oxide-functionalized PT have also been synthesized.<sup>117,118</sup> Some enhancement was also observed for PEDOT and PT,<sup>115</sup> because, as the Fermi level of the cyanide anion was close to that of the polymers used in the study, the anion served as a mediator for charge transfer between them<sup>119</sup>. Morphological changes in



poly(3-alkylthiophenes) have been linked to enhanced capacitance, conductivity, and stability.<sup>120</sup> A major concern is the lack of reliable synthetic methods for making large quantities of n-type polymer. In n-type polyfluorene stabilizing silicon nanoparticles in a composite anode,<sup>121</sup> the increased cycle life is attributed to reversible lithium doping in the polymer and the formation of an intimate composite. Furthermore, side-chain functionalization can be used to stabilize polythiophenes for n-doping.<sup>122</sup> Another concern is that diffusion limitations cause poor response times at high current densities with low power efficiencies. Self-doped polymers with ionic side chains help to provide fast response times and improved processability, but can suffer from low conductivities.<sup>123,124</sup> This can be alleviated to an extent by nanostructuring.<sup>124–126</sup> Overcoming diffusion limitations suggested that block copolymers of conducting PT and poly(ethylene oxide) were used to form films; the resulting material was successfully employed in a solid-state battery.<sup>127,128</sup>

## 2. Battery electrodes based on inorganic nanoparticle-conducting polymer composite

Inorganic nanoparticle–polymer composite electrodes are promising systems for secondary battery applications, due to their unusual combination of properties derived from the different building blocks. The flexibility and stability of composite electrodes arise from their polymer components and functionality. The general concept of designing a composite starts from a nanosized combination of polymers, metal particles and functional molecules. Composite materials are classified based on their interaction: (a) a functionalised polymer or metal precursor undergoes strong interaction *via* covalent and ionic bonds with amino-functionalised silicon nanoparticles and is polymerised<sup>129</sup> and (b) polymers embedded with inorganic nanoparticles, *e.g.* physical or chemical attachment of an iron complex to the backbone of a conducting polymer leads to stabilization of its charge/discharge characteristics and higher electrode capacities in LiFePO<sub>4</sub>.<sup>116</sup>

### 2.1. Materials synthesis

Nanostructured polymer–inorganic hybrid composites can often produce synergistic benefits based on their chemical composition and physical structure for applications as particular functional materials.<sup>116</sup> As the fastest-growing battery system, lithium ions (lithium-ion batteries) are used where high energy density and light weight are of prime importance. The device is fragile and a protection circuit is necessary to ensure safety.<sup>130</sup> Conducting polymers embedded with inorganic nanoparticles are suitable materials for high-performance electrodes in batteries due to their synergistic effects.<sup>131,132</sup> They provide good electrical conductivity, the polymer acts as a stress buffer and they promote transport of both electrons and ions owing to the availability of short diffusion paths and good connectivity. In addition, good

catalytic, magnetic, semiconducting and sensing properties, depending on the kind of nanoparticles and polymers and their characteristics, and the effects of the electrolyte concentration as well as the other reaction parameters on the morphology/properties of the final composite should be determined, controlled, improved and characterized in a very precise and careful manner during synthesis reactions.<sup>10,80</sup> Recently, several methods have also been employed for the synthesis of hybrid composites for different applications (see Table 3). Using facile one-step seeding-template-assisted oxidative polymerization reactions with different oxidizing agents, these are likely to generate core–shell or network-like composite structures that are composed of conducting polymers with different morphologies decorated with the abovementioned inorganic nanoparticles.<sup>133–137</sup> Within 0-D to 3-D matrices of these composites, unique “size-dependent” sensing properties and high catalytic ability were achieved. Furthermore, in hybrid composite electrodes, a considerable change in the shape, size, distribution, or connectivity of each phase during cycling may result in undesirable redistribution or segregation of phases. This may cause electrical isolation of active electrode materials (and so capacity fading), deteriorating connectivity between carbon particles (increased resistance to current collection and charge transfer), and a decline in transport of electroactive reactants to (or products from) active sites (increased resistance to mass transfer and reduced rate of charge and discharge). For example, in a change in morphology during charging, formation of lithium dendrites may cause partial shorting of the two electrodes and, eventually, complete failure of battery operation.<sup>138</sup> Several groups have proposed the synthesis of conducting polymers with silicon, tin, vanadium oxide nanoparticles, carbon, *etc.* Nazar *et al.*<sup>139</sup> and Buttry *et al.*<sup>140</sup> polymerized PANI in the presence of V<sub>2</sub>O<sub>5</sub> to make inorganic/organic hybrid electrodes. The Li<sup>+</sup> ion diffusion coefficient for the PANI/V<sub>2</sub>O<sub>5</sub> composite was 10 times that of V<sub>2</sub>O<sub>5</sub>, and the capacity was also superior to that of V<sub>2</sub>O<sub>5</sub> xerogel. Cui *et al.* carried out infusion of a PANI hydrogel into Si-based anodes: the hydrogel was polymerized *in situ*, resulting in a well-connected three-dimensional network structure consisting of SiNPs conformally coated by PANI. With this anode, a cycle life of 5000 cycles was demonstrated with over 90% capacity retention at 6.0 A g<sup>−1</sup> current density.<sup>13</sup> A SnNPs/PPy composite was prepared by chemically reducing and coating SnNPs onto a PPy surface. The composite has a much higher surface area than a pure nano-Sn reference sample, due to the higher surface area of porous PPy and the much smaller particle size of Sn in the nano-Sn/PPy composite than in the pure tin nanoparticle sample.<sup>141</sup> A polyaniline (PANI)/multi-walled carbon nanotube (CNT) composite cathode was prepared by *in situ* chemical polymerization of aniline in a well-dispersed CNT solution. The cell delivered a maximum discharge capacity of 86 mA h g<sup>−1</sup> at the 80<sup>th</sup> cycle with an average coulombic efficiency of 98%.<sup>142</sup> A secondary lithium metal battery modified by a PANI–CNT nanoporous composite buffer layer was fabricated to decrease the safety risk of the secondary Li metal battery in cycles of recharging processes and improve its cycle life in the future.<sup>143</sup>

Table 3 List of synthetic methods for conducting polymer–inorganic hybrid composites and their merits and demerits

Methods	Advantages	Disadvantages
<i>Ex situ</i> methods <sup>145</sup>	More suitable for large-scale industrial applications than the <i>in situ</i> method	The preparation of particles that possess higher dispersibility in the polymer and exhibit long-term stability against aggregation; in this process the dispersion of nanoparticles in the polymer matrix is difficult
<i>In situ</i> methods <sup>146</sup>	Prevents the agglomeration of inorganic particles while retaining good spatial distribution in the polymer matrix	The un-reacted products of the <i>in situ</i> reaction might influence the properties of the final materials
Mechanical methods <sup>154–159</sup>	The cost of power and a grinding medium is low; it is suitable for both batch and continuous operation and open- and closed-circuit grinding and applicable to materials of all degrees of hardness	Contamination, long processing time, no control of particle morphology, agglomerates, and residual strain in the crystallized phase
Blending inorganic nanoparticles into polymer matrix <sup>160–166</sup>	Reproducible fabrication with controlled levels of electrical conductivity, retaining the desired mechanical properties of the matrix, low-cost synthesis, avoiding oxidants or reductant chemicals	Difficulty in desired structure and properties, uniform low distribution of particles
Nanostructured polymer with inorganic particles <sup>167–173</sup>	Well-connected inorganic nanoparticles in polymers <i>via</i> chemical or physical bonding, soluble systems if they maintain their solubility after nanoparticle formation, potential use as thin films or free-standing films	Requires choice of the functional group to be introduced to polymers for interaction with inorganic particles
Sol–gel process <sup>175–184</sup>	This method provides good crystallinity, homogeneous mixing at the atomic or molecular level, low synthesis temperature, short heating time, good stoichiometric control, uniform particle size and small diameter down to the nanometer level	High shrinkage, low yield, high precursor costs, acidic gases evolved during pyrolysis, limited shelf life of sols
Surfactant-free solution processes <sup>199</sup>	Simple physical attraction process without external surfactants	Relatively poor control of uniformity of shape and diameter
Layer-by-layer <sup>200</sup>	Simple, cheap, and thin-film deposition method. Its important feature is the high degree of control over thickness, which arises due to linear growth of films with a number of bilayers	Slow deposition, waste of materials, and small surface areas
Self-assembly <sup>201</sup>	Large variety of shapes and functions on many length scales can be obtained	Synthesis more problematic due to the many free parameters that require control
Microemulsion polymerization method <sup>215</sup>	Enables fast polymerization rates without loss of temperature control, the viscosity of the reaction medium remains close to that of water, and the final product can be used as is and does not generally need to be altered or processed	An unwanted product is difficult to remove from the final composite and removal of water is an energy-intensive process for isolating composites
Template method <sup>222</sup>	Controllable length and diameter of nanotubes or wires	A post-synthetic process is needed to remove the template
Ion exchange process <sup>225</sup>	Reversible process which can be regenerated or loaded with desirable ions by washing with an excess of these ions	The final product formed can be dependent on the size of the ions, their charge, or their structure

## 2.2. *Ex situ* and *in situ* approaches

Most convenient and attractive routes to the fabrication of polymer composites embedded with inorganic nanoparticles (INPs) involve the following methods. In the *ex situ* approach, inorganic nanoparticles are first produced by soft-chemistry routes and then dispersed into polymeric matrices, whereas in the *in situ* approach metals are generated inside a polymer matrix by decomposition (*e.g.*, thermolysis, photolysis, radiolysis, *etc.*) or chemical reduction of a metallic precursor dissolved in the polymer. These types of polymer implanted with INPs have been extensively studied for energy and electrical

devices. The regulated porosity of polymers greatly affects the stability of electrodes in batteries. A porous polymer matrix has vacant space to allow a large expansion in volume and even assist cracked INPs trapped inside CPs with interconnected pores, and a highly conductive coating helps provide good electrical connectivity for INPs during discharge/charge. To enhance the lithium storage abilities of inorganic oxide-based anodes for LIBs, nanopainting with a thin layer of conducting polymer has been investigated.<sup>144</sup> A typical layered transition metal sulfide (MoS<sub>2</sub>) has a S–Mo–S layer with a structure similar to graphite together with van der Waals forces, which can

facilitate  $\text{Li}^+$  insertion/extraction. Poor conductivity between two adjacent S–Mo–S sheets can be improved by PANI *via* an *in situ* method to provide anode materials exhibiting high capacity and good cyclability for Li-ion batteries.<sup>145</sup>  $\text{LiFePO}_4$  particles generally have problems associated with slow diffusion of Li ions across the two-phase boundary and/or low conductivity, which were overcome by preparing a composite by an *in situ* polymerization restriction method, in which  $\text{Fe}^{3+}$  acts as a precipitating agent for  $\text{PO}_4^{3-}$  and an oxidant for aniline polymerization, and then coating it on graphite (1–2 nm). This material offered a good rate performance of  $80 \text{ mA h g}^{-1}$  at 60 C rate (Fig. 5).<sup>146</sup> Ding *et al.* proposed a new anode material  $\text{CoCO}_3$  using two-step conversion reactions with a total theoretical value of 7 Li per  $\text{CoCO}_3$ . The first reaction involves reduction of  $\text{CoCO}_3$  to metallic Co and formation of  $\text{Li}_2\text{CO}_3$  and the second reaction involves further reduction of  $\text{Li}_2\text{CO}_3$  to  $\text{Li}_x\text{C}_2$  ( $x = 0, 1, 2$ ), along with formation of  $\text{Li}_2\text{O}$ . The low stability of the electrode was increased by mixing it with PPy to form a  $\text{CoCO}_3$ –PPy composite, which exhibited remarkable cycling stability and reversibility, appearing to be a very promising anode material for LIBs (Fig. 5).<sup>147</sup> High-capacity Si and Sn anodes underwent huge volume expansion during cycling, which was controlled by PEDOT:PSS. This was embedded by *in situ* polymerization of EDOT in an aqueous solution of PSS with dispersed nanosized Si particles and subsequent carbonization of Si/PEDOT:PSS, which retained a specific capacity of  $768 \text{ mA h g}^{-1}$  and 99.2% CE after 80 cycles.<sup>148</sup> A nano-Sn–polypyrrole composite with CMC as binder displayed both superior capacity retention and good rate capability. It demonstrated that both CMC and polypyrrole (PPy) can act as composite binders and prevent the formation of cracks in electrodes during the charge–discharge process, resulting in good cycling stability, despite the large volume changes.<sup>141</sup> Generally, poor electronic conductivity of pristine anode and cathode materials hampers commercial applications. To improve electrode performance, conducting polymers are introduced by an *in situ/ex situ* preparation method. Arbizzani *et al.* introduced PEDOT onto  $\text{Li}_{1.03}\text{Mn}_{1.97}\text{O}_4$  by oxidation and subsequent polymerization of EDOT on

$\text{Li}_{1.03}\text{Mn}_{1.97}\text{O}_4$  particles promoted by itself, due to its oxidative property.<sup>149</sup> To improve the cycling process of a  $\text{LiMn}_2\text{O}_4/\text{Li}_x\text{V}_2\text{O}_5$  lithium-ion cell, coating with PPy on the surface of the anode was performed *via* an *in situ* polymerization method.<sup>150</sup> PANI was intercalated into  $\text{MnO}_2$ , which has a swollen layered structure, with uniform mesoporous structure, typical nano-size, and high surface area, resulting in high electrochemical performance for Li storage.<sup>151</sup> Enhanced electrochemical performance of  $\beta\text{-AgVO}_3/\text{PANI}$  triaxial nanowires was achieved *via* an *in situ* method.<sup>152</sup> A  $\text{V}_2\text{O}_5/\text{PPy}$  hybrid was prepared for improving performance by 20%.<sup>153</sup> The basic routes for preparation of hybrid composites are *in situ* synthesis of INPs, polymers or both components simultaneously. Mixture of final components or precursors can be obtained.

### 2.3. Mechanical methods

A grinder with high energy is used to crush material into extremely fine powder, which is known as the ball milling method. It is suitable for batch as well as continuous operation, materials of all degrees of hardness, and open- as well as closed-circuit grinding. The vast network of a PPy matrix is a suitable environment to buffer the volume change associated with  $\text{Li}_x\text{Si}$  alloying and dealloying reactions. The capacities of the composites were dependent on the amount of silicon added. A series of novel high-capacity Si/PPy composites was prepared by high-energy mechanical milling techniques.<sup>154</sup> Some 10 wt% PPy nanowires were introduced to Si particles prepared by high-energy mechanical milling to provide better reversibility and cycle life than for silicon, whereas a silicon/PPy microparticles composite displayed no improvement, because PPy NWs and PPy microparticles act as a matrix to hold active silicon grains as they repeatedly alloy with lithium during the operation of LIBs.<sup>155</sup> Metal oxides are semiconductors, which cannot provide higher capacity. However, mixing with polymers can deliver a reversible capacity more than ten times that of plain  $\text{MnO}_2$ -based devices. Reversible capacities were in the range  $400\text{--}1000 \text{ mA h g}^{-1}$  at  $120 \text{ mA g}^{-1}$  in the 20<sup>th</sup> cycle.<sup>156</sup> Furthermore, to enhance the long-term cyclability of a Si anode, SiNPs were embedded into a  $\text{Li}^+$ -conducting polymer (polyparaphenylene) (PPP) simply by ball-milling SiNPs with PPP as a core–shell structure, in which nano-Si cores act as an active Li storage phase and the polymeric matrix as a strong buffer to accommodate the volume change, as well as a protective barrier to prevent direct contact of the Si surface with the electrolyte. A Si/PPP composite exhibits a high capacity of  $3184 \text{ mA h g}^{-1}$  with 78% initial CE and  $1670 \text{ mA h g}^{-1}$  at  $16 \text{ A g}^{-1}$ , along with long-term cyclability, with 60% capacity retention over 400 cycles (Fig. 6).<sup>157</sup> More recently, high-capacity  $\text{VO}_4$  was synthesized from stoichiometric amounts of  $\text{In}_2\text{O}_3$  and  $\text{V}_2\text{O}_5$  in the ratio of 1 : 1 mixed using a ball mill for 18 h, which has a surface area of  $0.49$  to  $9.28 \text{ m}^2 \text{ g}^{-1}$  and a capacity about  $1200 \text{ mA h g}^{-1}$ .<sup>158</sup> A substantial change in shape during cycling, resulting in rapid capacity fading, has so far limited the success of this material. Composites that somehow remedy this detrimental effect have been studied, among these composites of silicon with PPy by Guo *et al.*<sup>159</sup>

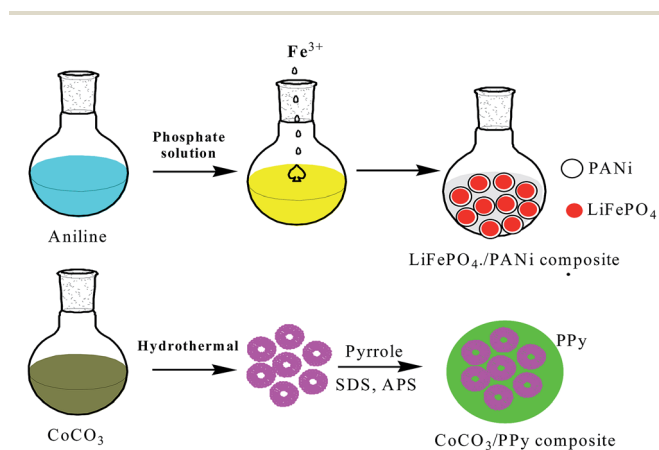


Fig. 5 Design of  $\text{LiFePO}_4/\text{carbon}$  and  $\text{CoCO}_3/\text{PPy}$  composites including an *in situ* polymerization reaction and two typical restriction processes.

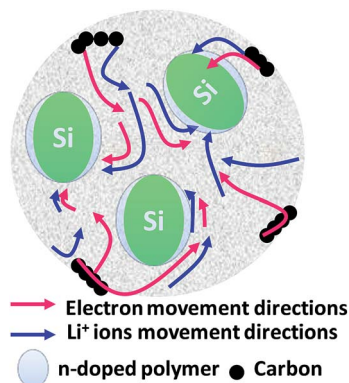


Fig. 6 Silicon nanoparticles with n-doped polymer for volume change buffering in nano-Si particles.

#### 2.4. Blending inorganic nanoparticles into polymer matrix

By simply pressing  $\text{LiMn}_2\text{O}_4$  and PPy powder without using any binder to give a pellet anode material at potentials ranging between 4.3 and 3.2 V vs.  $\text{Li/Li}^+$ , PPy works well as a conducting matrix for the redox reaction  $\text{LiMn}_2\text{O}_4 \rightleftharpoons \text{Li}_{1-x}\text{Mn}_2\text{O}_4 + x\text{Li}^+ + xe^-$ . PPy also behaved like a capacitor and contributed to the capacity density of the  $\text{LiMn}_2\text{O}_4$ /PPy composite.<sup>160</sup> A thin flexible polypyrrole–lithium iron phosphate (PPy– $\text{LiFePO}_4$ ) composite has been developed to enhance the electrical conductivity of the cathode (Fig. 7).<sup>161</sup> Deposition of PPy in hollow spherical crystalline  $\text{V}_2\text{O}_5$  yielded a composite with slightly reduced capacity but increased cycling stability.<sup>162</sup> PPy coated on small particles of  $\text{V}_2\text{O}_5$  evaluated as the positive mass of a lithium-ion battery by Zhao *et al.* displayed improved cyclability.<sup>163</sup> Using pyridine sulfonic acid as an additive during preparation of a  $\text{V}_2\text{O}_5$ /PPy hybrid material resulted in a capacity increase of 20%.<sup>164</sup> Differences between core/shell and host/guest nanocomposites of  $\text{V}_2\text{O}_5$ /PPy have been studied by Posudievsky *et al.*<sup>165</sup> Therefore, addition of a chemical oxidant and associated problems caused by an excess of this oxidant in the reaction system and possibly the final product could be avoided. The observed capacity of this positive mass was  $163 \text{ mA h g}^{-1}$ , which was close to the theoretical capacity of  $170 \text{ mA h g}^{-1}$  for  $\text{LiFePO}_4$ , with superior high-rate performance attributed to the improved lithium ion diffusivity of the composite material. The influence

of the morphology of  $\text{LiFePO}_4$  particles (donut-shape, dumbbell-shape, nanocrystalline) coated with PEDOT was studied by Dinh *et al.*<sup>166</sup>

#### 2.5. Nanostructured polymer with inorganic particles

Functional groups of polymers interact with inorganic salts and subsequent reduction or thermal (or other) treatment results in formation of nanoparticles within a functional nanophase. Capping, reducing, stabilising or protective agents (polymers, surfactants) play important roles during the formation of nanoparticles. Incorporation of a PANI–phytic acid hydrogel into Si-based anodes *via* hydrogen bonding followed by cross-linking resulted in a well-connected three-dimensional network structure consisting of SiNPs conformally coated by PANI. This anode demonstrated a cycle life of 5000 cycles with over 90% capacity retention at a current density of  $6.0 \text{ A g}^{-1}$ .<sup>11</sup> A  $\text{LiMn}_2\text{O}_4$ –PPy composite was studied for its charge–discharge properties at 3 V and 4 V (Scheme 5).<sup>167,168</sup> In order to improve electrode performance, pyrrole dispersed in  $\text{V}_2\text{O}_5$  forms a hybrid composite by a chemical polymerisation method, that can influence an acidic dopant<sup>169</sup>.  $\text{LiFePO}_4$  that was exposed to hot air and regenerated with PPy as a reductant was studied.<sup>170</sup> Excellent performance, in particular at high rates, was observed. This approach was further developed and optimized using EDOT as a monomer and its chemical oxidation by a slightly lithium-poor form of  $\text{LiFePO}_4$ .<sup>171</sup> Fabricated high-performance Li-ion battery anodes made by encapsulating SiNPs in a nanostructured 3D porous conductive polymer framework were developed.<sup>172</sup> A hierarchical conductive hydrogel framework with carbon nanotubes as an electronic promoter with high porosity was prepared to accommodate the Si particles of a SiNPs/PPy–CNT composite by *in situ* polymerization for improved cycling performance in LIBs.<sup>173</sup>

#### 2.6. Sol–gel method

Sol–gel methods are very attractive and instructive processes. They exhibit intense development accompanied by important practical applications in energy conversion and storage systems and possess significant advantages, for example, good crystallinity, homogeneous mixing at the atomic or molecular level, low synthesis temperature, short heating time, good

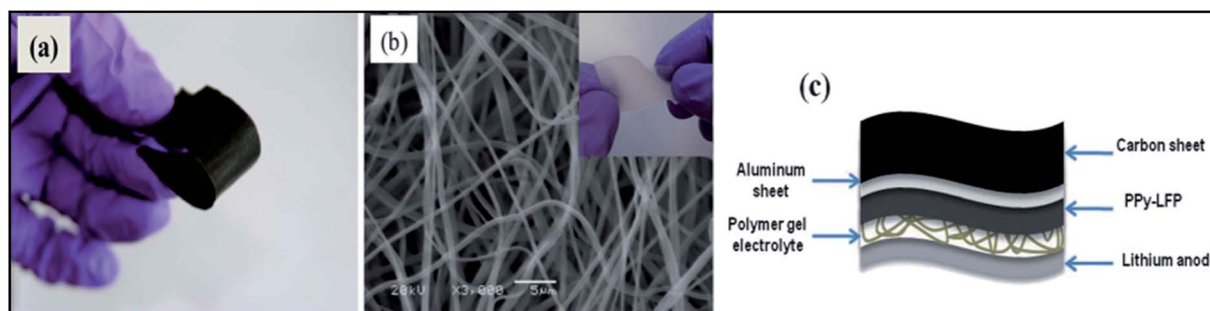
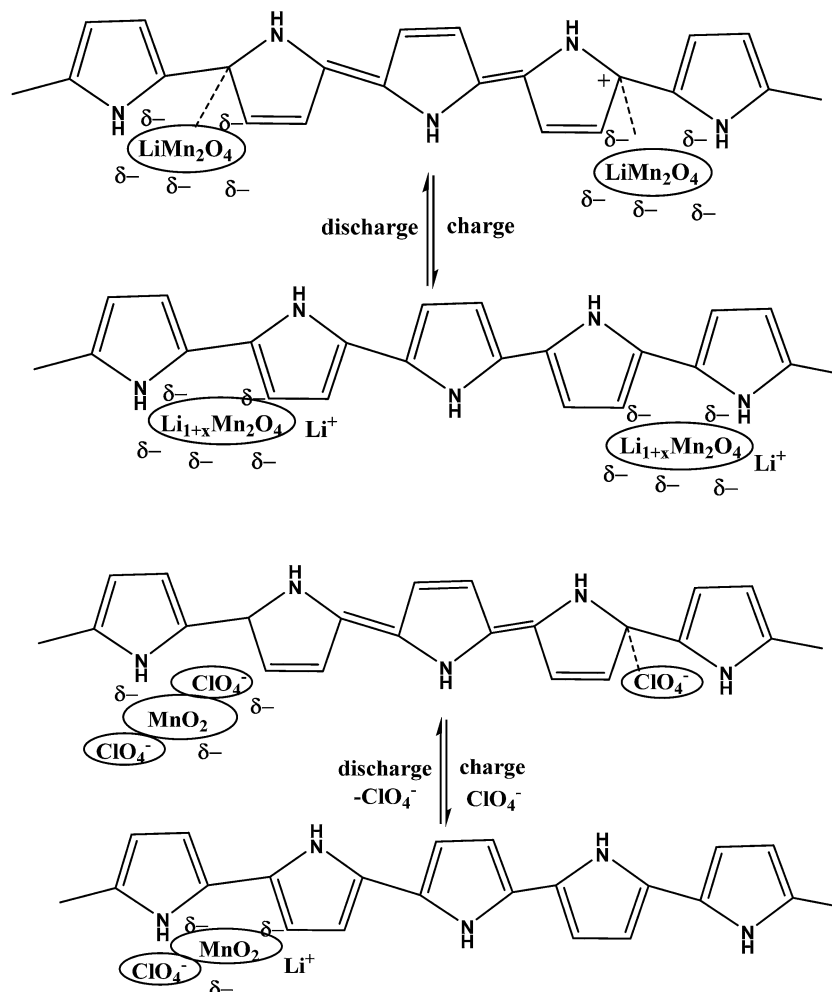


Fig. 7 Photograph (a) of a flexible PPy–LFP electrode, (b) SEM of electrospun P(VdF–HFP) matrix and (c) scheme of the flexible battery. Inset of (b) Photograph of electrospun P(VdF–HFP). (Reprinted with permission from ref. 161, copyright 2012, Royal Society and Chemical Journal).





Scheme 5 Schematic of changes in  $\beta\text{-MnO}_2/\text{PPy}$  (a) and  $\text{LiMn}_2\text{O}_4/\text{PPy}$  (b) in charge–discharge reactions.

stoichiometric control, uniform particle size and small diameter, down to the nanometer level.<sup>174</sup> The basic processing steps of this method are precursor, hydrolysis, reactive monomer, condensation, sol gelation, gel, and treatment. Controlled preparation of a  $\text{V}_2\text{O}_5/\text{PPy}$  composite led to favorable reversible electrochemical properties as suggested by Ren *et al.*<sup>175</sup> Furthermore,  $\text{V}_2\text{O}_5/\text{PPy}$  nanocomposites for  $\text{Li}^+$  ion transport were proposed.<sup>176,177</sup> A  $\text{V}_2\text{O}_5/\text{PPy}$  hydrogel composite was proposed for systematic studies of spectral and structural characterisation.<sup>178</sup> The electrochemical lithium intercalation properties of  $\text{V}_2\text{O}_5/\text{PANI}$  were studied.<sup>179,180</sup> Park *et al.* deposited  $\text{V}_2\text{O}_5$  on a layer of PANI.<sup>181</sup>  $\text{Li}_4\text{Ti}_5\text{O}_{12}$  was prepared by the sol–gel method, followed by coating with PANI, and exhibited better rate capability and cyclability.<sup>182</sup> Tethering a carbon-coated  $\text{LiFePO}_4/\text{PPy}$  composite demonstrated enhancement of the rate capability of cathode composites.<sup>183</sup> Core/shell structures prepared from small crystals of  $\text{V}_2\text{O}_5$  coated with PPy were inferior to host/guest structures synthesized from an aerogel of  $\text{V}_2\text{O}_5$  with mechanochemical polymerization of pyrrole. Nanocomposites of PEDOT and  $\text{V}_2\text{O}_5$  prepared with microwave assistance displayed an increased capacity of  $370 \text{ mA h g}^{-1}$ .<sup>184</sup>

## 2.7. Electrochemical and chemical deposition methods

A thin film is a layer of material ranging from fractions of a nanometer (monolayer) to several micrometers in thickness. Electronic semiconductor devices and optical coatings are the main applications benefiting from thin-film construction. Polymer composite electrodes are mostly synthesized by deposition methods such as chemical or electrochemical processes. A  $\text{LiFePO}_4$  electrode is modified with PPy *via* monomer penetration and coating in inner pores, which would reduce surface activity and further decrease undesirable reactions with the electrolyte, while lithium intercalation would not be inhibited. This strategy is used to synthesize PPy films.<sup>185</sup> Si/PPy core–shell nanofibers obtained by electropolymerization of a PPy nanofibers electrode followed by CVD of SiNPs are favorable for facile charge delivery and gathering, whereas the porosity of the electrode can efficiently buffer the volume expansion of Si (Fig. 8).<sup>186</sup> By electrochemical deposition, PPy-doped  $\text{LiFePO}_4$  cathodes were prepared, and displayed poor electrochemical properties.<sup>187–190</sup> Huang *et al.* reported a porous NiO/polyaniline (PANI) film obtained by depositing a PANI layer on the surface of a NiO film, which exhibited a capacity of  $520 \text{ mA h g}^{-1}$  at

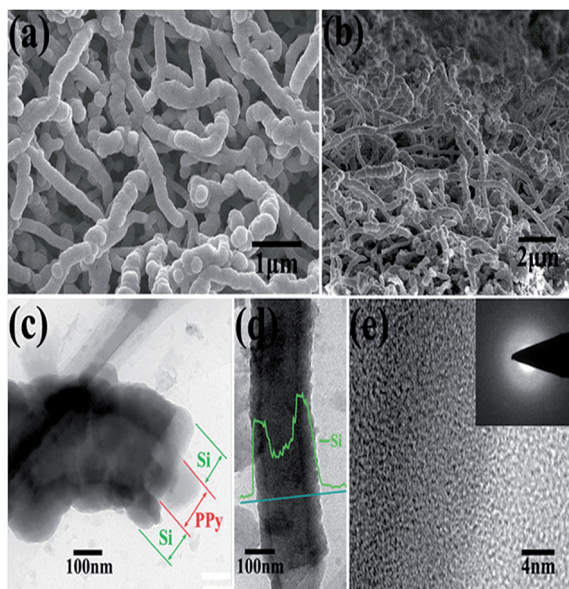
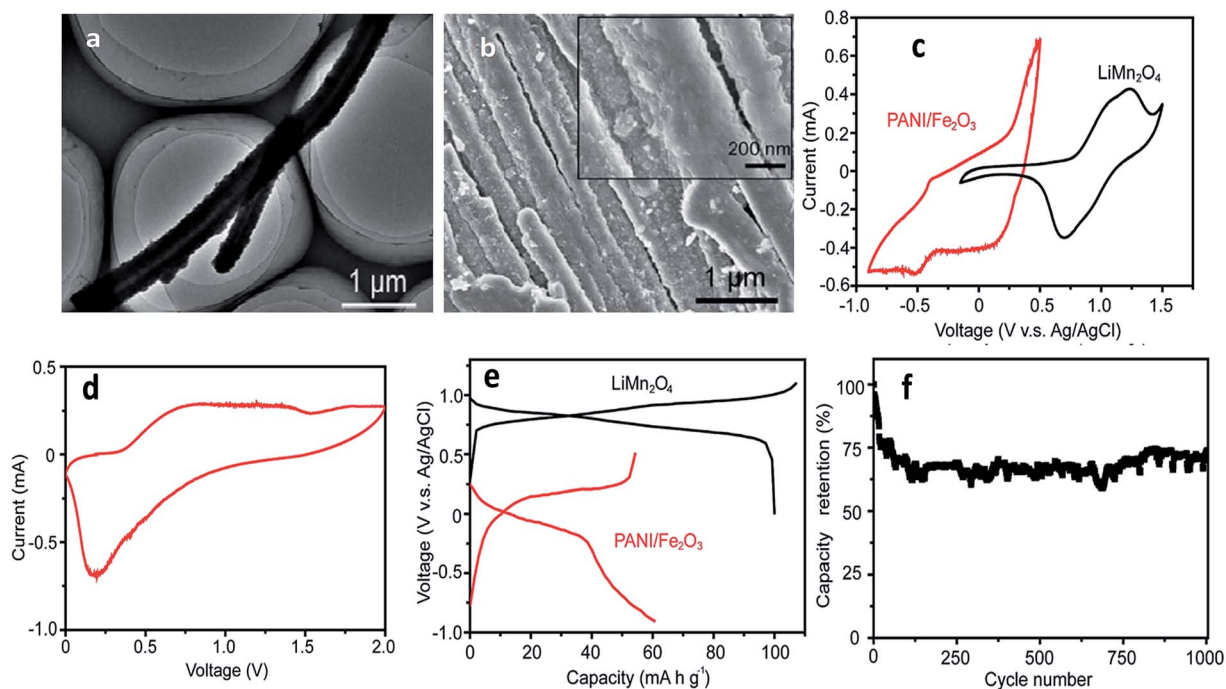


Fig. 8 (a) and (b) top and cross-sectional SEM images of PPy-Si core-shell nanofiber network after Si deposition. (c) and (d) TEM images of the core-shell structure of Si@PPy nanocables. (e) High-resolution TEM image of Si coatings. Inset of (e) SAED image of Si coatings (reprinted with permission from ref. 186, copyright 2012, Royal Society and Chemical Journal).

1 C.<sup>191</sup> Porous NiO/PEDOT films are prepared by chemical bath and electrodeposition techniques and exhibit weaker polarization and better cycling performance.<sup>192</sup> Free-standing PPy/LiFePO<sub>4</sub> film electrodes were prepared using the same solution, but with the addition of LiFePO<sub>4</sub> powder. A cell with a composite film displayed a higher discharge capacity beyond 50 cycles (80 mA h g<sup>-1</sup>) than that of a cell with pure PPy (60 mA h g<sup>-1</sup>).<sup>193</sup> Wang *et al.* prepared by an electrochemical method highly flexible, paper-like, free-standing PPy and PPy-LiFePO<sub>4</sub> composite film electrodes and observed that a cell with PPy-LiFePO<sub>4</sub> composite film exhibited a higher discharge capacity beyond 50 cycles (80 mA h g<sup>-1</sup>) than that of a cell with pure PPy (60 mA h g<sup>-1</sup>).<sup>194</sup> LiFePO<sub>4</sub>, as a typical compound affected by conductance problems, was coated with carbon and embedded in PPy during electropolymerization of the latter compound. Improved specific capacity and rate behavior were reported, with the capacitance attributed to substitution of the inactive carbon matrix (and binder) by redox-active PPy and the rate improvement attributed to the vastly increased electronic conductance of the matrix. Carbon-coated particles of LiFePO<sub>4</sub> were tethered to PPy by Huang *et al.*<sup>195</sup> A substantial change in shape during cycling, which resulted in rapid capacity fading, has so far limited the success of this material. Composites that somehow remedy this detrimental effect have been studied, such as silicon with PPy.<sup>196</sup> A high-capacity LIB anode SiNWs/PEDOT material was formulated by an electropolymerisation method, which maintained the mechanical integrity of the cycled Si material, along with preserving electrical connections between NWs that would otherwise have become electrically isolated during volume changes.<sup>197</sup>

## 2.8. Miscellaneous methods

A Fe<sub>2</sub>O<sub>3</sub>-decorated polyaniline (PANI/Fe<sub>2</sub>O<sub>3</sub>) multi-channelled nanotube structure as an anode for an aqueous rechargeable lithium-ion battery (ARLIB) was made using polymerized aniline-Mo<sub>3</sub>O<sub>10</sub> nanowires as a template. The removal of MoO<sub>x</sub> from intercalated layered MoO<sub>x</sub>/PANI structures results in a multi-channelled nanotube structure. Subsequent hydrothermal growth of Fe<sub>2</sub>O<sub>3</sub> nanoparticles on the surface of PANI can simultaneously re-dope PANI to provide a highly conductive form, while the surfaces of PANI become relatively smooth, and growth of Fe<sub>2</sub>O<sub>3</sub> is observed on the surface of the PANI/Fe<sub>2</sub>O<sub>3</sub> nanocomposites, where the number of channels in each NT ranges from 2 to 5 (Fig. 9a and b). Study of CVs indicates deintercalation of Li<sup>+</sup> at the available tetrahedral sites, and the cathodic curve shows the reverse process. The initial discharge and charge capacities of the PANI/Fe<sub>2</sub>O<sub>3</sub> multi-channelled nanotube anode are 60.5 and 54.2 mA h g<sup>-1</sup> at 150 mA g<sup>-1</sup>, respectively. When fabricated as an ARLIB full cell with the PANI/Fe<sub>2</sub>O<sub>3</sub> multi-channelled nanotube anode and a LiMn<sub>2</sub>O<sub>4</sub> cathode, an initial discharge capacity of 50.5 mA h g<sup>-1</sup> is obtained at a current rate of 150 mA g<sup>-1</sup>, with superior capacity retention of 73.3% after over 1000 charge/discharge cycles (Fig. 9c-f).<sup>198</sup> Iron species attached physically or chemically to the backbone of PPy comprising LiFePO<sub>4</sub> lead to stabilization of its charge/discharge characteristics and higher electrode capacities.<sup>116</sup> Se/PPy/graphene composites were synthesized by surfactant-free solution processes and exhibit a large discharge capacity of 678 Ah kg<sup>-1</sup> at a current rate of C/120 when used as a Li-Se battery.<sup>199</sup> Layer-by-layer assembly was used to improve the characteristic properties of V<sub>2</sub>O<sub>5</sub> and PANI with a volumetric charge density of 264 mA h cm<sup>-3</sup>.<sup>200</sup> When PANI was deposited by a self-assembly process onto carbon particles with LiFePO<sub>4</sub>, it was found that capacity increased, in particular at high rates.<sup>201</sup> PPy-covered NiO was used to remedy the problems inherent in volume change.<sup>202</sup> PPy can also be used to reduce charge transfer resistance associated with the Li<sup>+</sup> ion intercalation/deintercalation reaction such as in PPy/MoO<sub>3</sub>, PPy/V<sub>2</sub>O<sub>5</sub>, PPy/LiCoO<sub>2</sub> and PPy/LiV<sub>3</sub>O<sub>8</sub>.<sup>203-207</sup> Javier *et al.* found that the theoretical capacity value of LiFePO<sub>4</sub> was maintained using a block copolymer of poly(3-hexylthiophene) and poly(ethylene oxide).<sup>208</sup> An α-LiFeO<sub>2</sub>-PPy nanocomposite was prepared by a chemical polymerization method as a cathode material to improve reversible capacity and cycling stability (104 mA h g<sup>-1</sup> at 0.1 C after 100 cycles).<sup>209</sup> To prevent contact of the nano-Si surface with the electrolyte, SiNPs were covered by a Li<sup>+</sup>-conducting polymer matrix, thus suppressing the continual rupturing and re-formation of SEI films on the Si surface.<sup>210</sup> Han *et al.* discovered a multifunctional PPy/Fe<sub>2</sub>O<sub>3</sub>/C nanostructure as a stable and highly efficient anode.<sup>211</sup> Controlled Li<sup>+</sup> diffusion in anode materials was obtained from SnO<sub>2</sub>/PPy nanocomposites.<sup>212,213</sup> The conductivity of SiNPs was significantly improved by PPy to prevent cracking of the electrode during cycling.<sup>214</sup> A microemulsion polymerization method was used for a SnO<sub>2</sub>/PANI composite in anode material applications.<sup>215</sup> SnO<sub>2</sub>-based composite coaxial nanocables with carbon-related particles (MWCNT, graphene, SWNT) anchored on conducting



**Fig. 9** (a) TEM image of a representative re-doped PANI NT, (b) SEM image of PANI/Fe<sub>2</sub>O<sub>3</sub> NTs. Inset: NT surface at a higher magnification, (c) cyclic voltammograms of PANI/Fe<sub>2</sub>O<sub>3</sub> NTs and commercial LiMn<sub>2</sub>O<sub>4</sub> in the first cycle at a scanning rate of 1 mV s<sup>-1</sup>, (d) cyclic voltammogram of ARLIB, which is assembled using PANI/Fe<sub>2</sub>O<sub>3</sub> and commercial LiMn<sub>2</sub>O<sub>4</sub> as anode and cathode, respectively, in the first cycle at a scanning rate of 1 mV s<sup>-1</sup>, (e) initial charge and discharge curves of PANI/Fe<sub>2</sub>O<sub>3</sub> NTs and commercial LiMn<sub>2</sub>O<sub>4</sub> at a current rate of 100 mA g<sup>-1</sup> and (f) capacity retention of the (PANI/Fe<sub>2</sub>O<sub>3</sub>)/LiMn<sub>2</sub>O<sub>4</sub> ARLIB full cell at a current rate of 150 mA g<sup>-1</sup> (reprinted with permission from ref. 198, copyright 2014, Royal Society and Chemical Journal).

polymers exhibited excellent stability and high reversible capacity.<sup>216–220</sup> TiO<sub>2</sub>-based conducting polymer composites synthesized by hydrothermal and chemical polymerization methods were developed to enable fast discharge and charge with enhanced electrochemical performance.<sup>219–221</sup>

Utilization of a template in the synthesis of core-shell CuO/PPy composites led to improved stability, electrical conductivity and electrochemical performance.<sup>222</sup> Surface adsorption of PDDA on LiMn<sub>2</sub>O<sub>4</sub> particles extended the lifetime of a LIB by retarding dissolution of Mn<sup>+</sup>, thus increasing the stability of the battery.<sup>223</sup> The improved electrochemical performance of a NiO/PPy composite was also studied.<sup>224</sup> A cation exchange technique was used for a high-performance cathode material (PPy/VO<sub>x</sub>-NTs).<sup>225</sup> Dissolution of a metal oxide on a LiNi<sub>1/3</sub>Mn<sub>1/3</sub>Co<sub>1/3</sub>O<sub>2</sub>/Li<sub>x</sub>V<sub>2</sub>O<sub>5</sub>/PANI composite was studied.<sup>226</sup> Surface coating of PPy on LiFePO<sub>4</sub> particles was carried out to improve their electronic conductivity.<sup>227</sup> A mixed ion/electron conductor comprising PPy with PAAMPSPA was used as an additive in sulfur cathodes in Li-S batteries.<sup>228</sup> Nest-like PANI-coated SiNPs were also proposed.<sup>229</sup> When the reverse micelle approach to V<sub>2</sub>O<sub>5</sub>/PANI was analyzed, the hybrid material seemed to stabilize the capacity due to a probable homogeneous distribution of the stress induced during cycling.<sup>230</sup> A simple mixture of a conductive binder (SPAN) and ramsdellite MnO<sub>2</sub> was used as a cathodic material for a lithium polymer battery.<sup>231</sup> A concomitant ion exchange and polymerization method was used in MoO<sub>3</sub>/PANI, which provided a moderate increase in cell

capacity and improved the reversibility of the Li insertion reaction.<sup>232</sup> An organic-inorganic hybrid material was formed from PANI/hexacyanoferrate (HCF) anion; anchoring of the electroactive anion within the polymer caused its application as a functional material that harnessed the activity of the molecular species.<sup>233</sup> A pressurized method was used for the synthesis of SnNPs/PANI which was examined for anode properties.<sup>234</sup>

### 2.9. Influencing the capacity, rate and life cycle

To operate a real battery, its capacity, charging rate and cycle life are very significant factors. They are associated with volume expansion, surface degradation and dissolution of active material. High-capacity lithium-ion anode materials always lead to problems with volume change and swelling after the electrodes absorb lithium because the structural integrity of the electrode has changed. Many anode materials swell to more than three times their volume when fully charged. Many methods have been suggested to solve this volume change issue. Also, metal nanoparticles need high volumes of a conductive additive (carbon) to ensure conductivity within the particle, which may reduce capacity and provide no mechanical binding force. Flexible conducting polymers can withstand large strain and maintain their conductivity as well as mechanical integrity. Recently, an n-type CP was synthesized and applied as a conductive binder in LIBs. This tailored the energy levels of polymer conduction, which helped provide adequate conductivity, and easily mechanically adhered to a Si



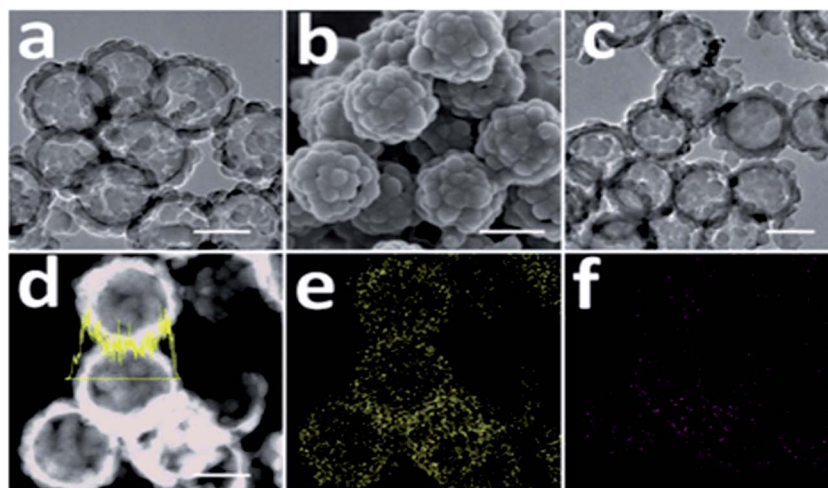


Fig. 10 (a) TEM image of T-HSSP, (b) SEM image of T-HSSP, (c) TEM image of S@PPy-300 composite, (d) STEM image and line scan analysis (sulfur) of S@PPy-300 composite, (e) elemental mapping of sulfur in (d) and (f) elemental mapping of carbon in (d). All scale bars: 200 nm (reprinted with permission from ref. 244, copyright 2014, Royal Society and Chemical Journal).

particle surface. Electrodes based on polyaniline and PVDF exhibited poor performance due to the insulating nature of the polymer matrix, whereas Si/AB/PVDF and Si/PFFO electrodes display high initial capacity but rapid loss. PFFOMB achieved intimate electrical contact for electron conduction and mechanical integrity with the desired electronic and mechanical properties and provided good specific capacity and stable cycling performance of  $2100 \text{ mA h g}^{-1}$  for Si and  $1400 \text{ mA h g}^{-1}$  for the electrode after 650 cycles. An isosurface study indicates that electron doping from lithium to PF-type conductive polymers (PFFO) is almost complete, with different LUMO and LUMO + 1. However, for polyaniline, there is strong lithium s- and polyaniline p-hybridization with limited charge transfer. Therefore, an electron is almost completely donated to PFFO once lithium is bound to the carbonyl site of the polymer.<sup>235</sup> SnNPs can be cycled with stable high gravimetric capacity ( $>500 \text{ mA h g}^{-1}$ ) with a polyfluorene-type conductive polymer binder in composite electrodes due to them offering electrical conductivity and strong adhesion during volume change.<sup>236</sup> The enhanced cycling stability of a conductive polymer-Si composite is related to the mesoscale synergistic functions of SiNPs and the conductive polymer. *In situ* TEM shows volume changes controlled by CPs which helped increase Li ion diffusion.<sup>237</sup> A multifunctional conductive polymer binder helped maintain high electronic conductivity, mechanical adhesion, ductility, and electrolyte uptake.<sup>238</sup>

To reduce the charging time, high-rate and high-voltage materials have been used. A core-shell structure of PEDOT and  $\text{V}_2\text{O}_5$  with graphite foam was formulated for ultra-fast stable Li-ion storage performance, with higher capacities and improved rate ( $168 \text{ mA h g}^{-1}$  at 60 C) and cycling capabilities.<sup>239</sup> Iron oxide capped with PANI demonstrates a high rate capability and a high capacity of  $778 \text{ mA h g}^{-1}$  was retained at a higher current rate of  $1.0 \text{ A g}^{-1}$  after 100 cycles.<sup>240</sup> PPy/PEG-modified sulfur/CNTs were synthesized using an *in situ* polymerization method and, remarkably, the battery could work at a

very high current density of  $8 \text{ A g}^{-1}$  and retained a capacity of  $480 \text{ mA h g}^{-1}$  after 100 cycles.<sup>241</sup> High rates of charge and discharge of a battery were achieved by substitution of a conductive electroactive polymer on  $\text{LiFePO}_4$ .<sup>242</sup> High rate capability of SiNPs was achieved using a PEDOT/PSS/CNT matrix, which possessed a three-dimensionally interconnected

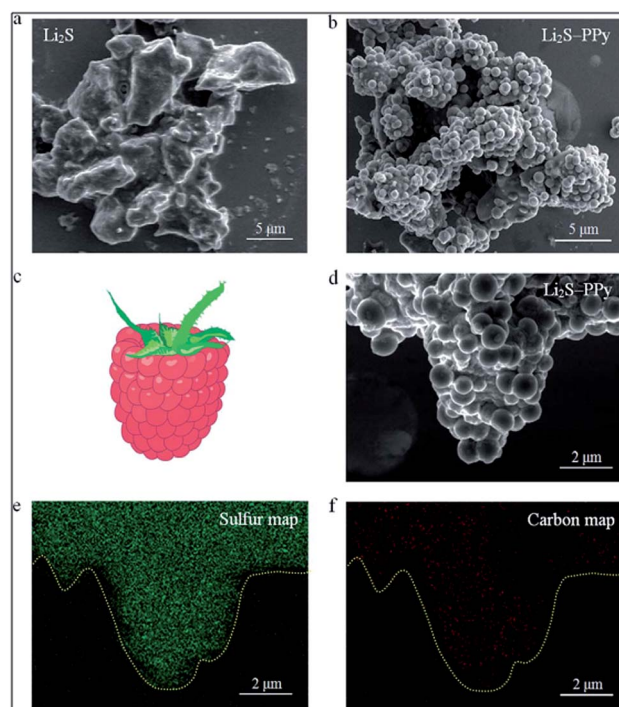


Fig. 11 SEM images of (a) pristine  $\text{Li}_2\text{S}$  particles and (b) as-synthesized  $\text{Li}_2\text{S}$ -PPy composite structures. (c) Schematic of a raspberry and (d) SEM image of a representative  $\text{Li}_2\text{S}$ -PPy raspberry-like composite together with the corresponding elemental maps for (e) sulfur and (f) carbon (reprinted with permission from ref. 246, copyright 2014, Royal Society and Chemical Journal).



hybrid hydrogel system and was able to retain a capacity of 1200 mA h g<sup>-1</sup> at a rate of 4.2 A g<sup>-1</sup>.<sup>243</sup> Thin-walled hollow spherical-structured PPy with sulfur which can buffer the volume expansion during charge/discharge have been proposed for Li-S batteries (Fig. 10).<sup>244</sup>

Long-term cycling of an electrode in a real battery is highly dependent on volume expansion and surface degradation of materials. If these factors are well controlled, the battery will function successfully for a long time. A CuHCF cathode and C/PPy anode combined into a full cell displayed good long-term cycling with 100% CE at a 50 C rate after 1000 cycles.<sup>245</sup> Cui *et al.* reported incorporation of a PANI hydrogel into Si-based anodes *via* an *in situ* method, resulting in a well-connected 3D network structure which consisted of SiNPs conformally coated by PANI. This exhibited a cycle life of 5000 cycles with over 90% capacity retention at 6.0 A g<sup>-1</sup>.<sup>13</sup> Strong binding of PPy onto the surface of Li<sub>2</sub>S helps limit intermediate Li<sub>2</sub>Sn species during cycling and provided a long cycle life (400 cycles). Fig. 11 shows scanning electron microscopy (SEM) images of Li<sub>2</sub>S particles coated with PPy, the formation of multiple PPy nanocolloids (700 nm) over the surface of the Li<sub>2</sub>S particles, and the appearance of a raspberry-like Li<sub>2</sub>S-PPy composite structure.<sup>246</sup> A membrane-assisted precipitation technique was used for S/PEDOT nanocomposites and controls the volume expansion for Li-S batteries.<sup>247</sup>

### 3. Summary and outlook

LIBs are in demand for powering technologies for today's portable electronics. However, these batteries have lacked commercial success because of their low stability, high cost, and relatively low energy and power density. These problems had traditionally been addressed *via* characterization of electrodes, electrolytes, and conductive or binder materials. Inorganic particles with polymers are a much-needed vibrant area of chemical research that has offered the opportunity to design innovative energy storage materials for higher capacity and longer cycle life of LIBs. Inorganic-polymer nanocomposites possess a high surface area, which can provide high Li<sup>+</sup> ion flux across the electrode interface, short diffusion pathways for Li ions and electrons, abundant active sites for Li storage, and high tolerance for volume change during charge/discharge to enhance the structural stability of the electrodes. Many kinds of chemical reactions have been reported on nanocomposites that include both organic conducting polymers and metal particles using addition and exchange methods. The resulting materials have exhibited new electrochemical properties relevant to storage and catalysis applications. The growth in interest and improved success no doubt coincides with the development of nanocomposites, which provide higher surface areas, improved oxidation/reduction kinetics, and better charge storage and continue to play an important role in many clinical, environmental, industrial, pharmaceutical, defense, and security applications due to their superior properties.

Battery electrodes based on inorganic-polymer nanocomposites offer high capacity, the possibility of long-term stability, and a low-cost, simple and reproducible fabrication

method, and as such they require a renewed approach to their design and development. Furthermore, this will promote the development of useful and reliable battery devices. However, certain limitations and uncertainty regarding poor safety, reduced capacity, poor rate capability and conductivity are the biggest difficulty with batteries. Also, there is a need to understand the Li storage mechanisms of materials, kinetic transport at the electrode/electrolyte interface, and the development of extrapolating theoretical tools for a better fundamental understanding of the relationships between nanocomposites and their electrochemical properties. Future directions in electrode materials should focus on the search for new electrodes and the design of structures and morphology for improved power density, rate capability, service life, and safety and reduced cost. More sustainable and greener methods should be adopted for producing high-power batteries, which will limit pollution and secure a future for living systems.

### Acknowledgements

We thank CRK Rao and M. Vijayan at CSIR labs of ICT and CECRI, respectively, for helpful guidance. One author (Prakash Sengodu) expresses his hearty thanks to Ms Mamali Das for supportive discussion. The authors also thank reviewers for providing valuable suggestions and making a quality paper.

### Notes and references

- 1 G. A. Nazri and G. Pistoia, *Lithium Batteries Science and Technology*, Springer, 1st edn, 2003.
- 2 W. A. Schalkwijk and B. Scrosati, *Advances in Lithium-Ion Batteries*, Kluwer Academic/Plenum Publishers, 1st edn, 2002.
- 3 R. A. Huggins, *Advanced Batteries Materials Science Aspects*, Springer, 2008.
- 4 M. V. Reddy, G. V. Subba Rao and B. V. R. Chowdari, *Chem. Rev.*, 2013, **113**, 5364–5457.
- 5 B. Nicolas, *Focus on the US Batteries Market*, US Reuters, 5 February 2009.
- 6 M. S. Islam and C. A. J. Fisher, *Chem. Soc. Rev.*, 2014, **43**, 185.
- 7 B. Dunn, H. Kamath and J. M. Tarascon, *Science*, 2011, **334**, 928.
- 8 X. Gao, W. Luo, C. Zhong, D. Wexler, S. L. Chou, H. K. Liu, Z. Shi, G. Chen, K. Ozawa and J. Z. Wang, *Sci. Rep.*, 2014, **4**, 6095.
- 9 K. C. White, *US patent* no US20100124702 A1, US 12/272,157, 2010.
- 10 S. Prakash, T. Chakrabarty, A. K. Singh and V. K. Shahi, *Biosens. Bioelectron.*, 2013, **41**, 43.
- 11 P. G. Bruce, B. Scrosati and J. M. Tarascon, *Angew. Chem., Int. Ed.*, 2008, **47**, 2930.
- 12 A. S. Aricò, P. Bruce, B. Scrosati, J. M. Tarascon and W. Van Schalkwijk, *Nat. Mater.*, 2005, **4**, 366.
- 13 N. Liu, W. Li, M. Pasta and Y. Cui, *Front. Phys.*, 2013, **9**, 323.
- 14 B. Liu, P. Soares, C. Checkles, Y. Zhao and G. Yu, *Nano Lett.*, 2013, **13**, 3414.

- 15 S. Prakash, C. R. K. Rao and M. Vijayan, *Electrochim. Acta*, 2009, **54**, 5704.
- 16 S. Prakash, C. R. K. Rao and M. Vijayan, *Electrochim. Acta*, 2008, **53**, 5919.
- 17 D. Wei, D. Cotton and T. Ryhanen, *Nanomaterials*, 2012, **2**, 268.
- 18 G. Wallace, T. Campbell and P. Innis, *Fibers Polym.*, 2007, **8**, 135.
- 19 S. Trohalaki, *MRS Bull.*, 2012, **37**, 883.
- 20 H. Wu, G. Zheng, N. Liu, T. J. Carney, Y. Yang and Y. Cui, *Nano Lett.*, 2012, **12**, 904.
- 21 K. Bock, *Proc. IEEE*, 2005, **93**, 1400.
- 22 H. E. Katz, P. C. Searson and T. O. Poehler, *J. Mater. Res.*, 2010, **25**, 1561.
- 23 M. E. Abdelhamid, A. P. OMullane and G. A. Snook, *RSC Adv.*, 2015, **5**, 11611–11626.
- 24 G. A. Snook, P. Kao and A. S. Best, *J. Power Sources*, 2011, **196**, 1.
- 25 S. R. Forrest, *Nature*, 2004, **428**, 911.
- 26 T. Tsutsui and K. Fujita, *Adv. Mater.*, 2002, **14**, 949.
- 27 A. Ueda, M. Nagao, A. Inoue, A. Hayashi, Y. Seino, T. Ota and M. Tatsumisago, *J. Power Sources*, 2013, **244**, 597.
- 28 Q. Sun, X. Q. Zhang, F. Han, W. C. Li and A. H. Lu, *J. Mater. Chem.*, 2012, **22**, 17049.
- 29 J. Yin, H. Cao, Z. Zhou, J. Zhang and M. Qu, *J. Mater. Chem.*, 2012, **22**, 23963.
- 30 L. Shao, J. W. Jeon and J. L. Lutkenhaus, *Chem. Mater.*, 2011, **24**, 181.
- 31 Y. H. Huang and J. B. Goodenough, *Chem. Mater.*, 2008, **20**, 7237.
- 32 G. Liu, S. Xun, N. Vukmirovic, X. Song, O. P. Velasco, H. Zheng, V. S. Battaglia, L. Wang and W. Yang, *Adv. Mater.*, 2011, **23**, 4679.
- 33 B. Scrosati and J. Garche, *J. Power Sources*, 2010, **195**, 2419.
- 34 D. A. Pasquier, I. Plitz, S. Menocal and G. Amatucci, *J. Power Sources*, 2003, **115**, 171.
- 35 M. Dubarry and B. Y. Liaw, *J. Power Sources*, 2009, **194**, 541.
- 36 R. Bittihn, G. Ely, F. Woeffler, H. Munstedt, H. Naarmann and D. Naegele, *Makromol. Chem., Macromol. Symp.*, 1987, **8**, 51.
- 37 J. Chen, J. Wang, C. Wang, C. O. Too and G. G. Wallace, *J. Power Sources*, 2006, **159**, 708.
- 38 K. Kaneto, K. Yoshino and Y. Inuishi, *Jpn. J. Appl. Phys.*, 1983, **22**, L567.
- 39 C. Arbizzani, M. Mastragostino and M. Rossi, *Electrochem. Commun.*, 2002, **4**, 545.
- 40 J. C. Carlberg and O. Inganas, *J. Electrochem. Soc.*, 1997, **144**, L61.
- 41 L. Shao, J. W. Jeon and J. L. Lutkenhaus, *Chem. Mater.*, 2011, **24**, 181.
- 42 T. F. Otero and I. Cantero, *J. Power Sources*, 1999, **81**, 838.
- 43 J. M. Kim, H. S. Park, J. H. Park, T. H. Kim, H. K. Song and S. Y. Lee, *ACS Appl. Mater. Interfaces*, 2014, **6**, 12789.
- 44 G. Kucinskis, G. Bajars and J. Kleperis, *J. Power Sources*, 2013, **240**, 66.
- 45 D. Deng, M. G. Kim, J. Y. Lee and J. Cho, *Energy Environ. Sci.*, 2009, **2**, 818.
- 46 M. R. Zamfir, H. T. Nguyen, E. Moyon, Y. H. Lee and D. Pribat, *J. Mater. Chem. A*, 2013, **1**, 9566.
- 47 S. L. Chou, Y. Pan, J. Z. Wang, H. K. Liu and S. X. Dou, *Phys. Chem. Chem. Phys.*, 2014, **16**, 20347.
- 48 P. Novak, O. Haas, K. S. V. Santhanam and K. Muller, *Chem. Rev.*, 1997, **97**, 207.
- 49 S. B. Chikkannanavar, D. M. Bernardi and L. Liu, *J. Power Sources*, 2014, **248**, 91.
- 50 V. Aravindan, J. Gnanaraj, Y. S. Lee and S. Madhavi, *J. Mater. Chem. A*, 2013, **1**, 3518.
- 51 J. O. Besenhard, J. Yang and M. Winter, *J. Power Sources*, 1997, **68**, 87.
- 52 C. K. Chan, H. L. Peng, G. Liu, K. McIlwrath, X. F. Zhang, R. A. Huggins and Y. Cui, *Nat. Nanotechnol.*, 2008, **3**, 31.
- 53 M. T. McDowell, S. W. Lee, C. Wang and Y. Cui, *Nano Energy*, 2012, **1**, 401.
- 54 H. Wu and Y. Cu, *Nano Today*, 2012, **7**, 414.
- 55 L. Qie, L. X. Yuan, W. X. Zhang, W. M. Chen and Y. H. Huang, *J. Electrochem. Soc.*, 2012, **159**, A1624.
- 56 W. M. Chen, L. Qie, L. X. Yuan, S. A. Xia, X. L. Hu, W. X. Zhang and Y. H. Huang, *Electrochim. Acta*, 2011, **56**, 2689.
- 57 G. Zhang, X. Li, H. Jia, X. Pang, H. Yang, Y. Wang and K. Ding, *Int. J. Electrochem. Sci.*, 2012, **7**, 830.
- 58 K. Park, H. Song, Y. Kim, Y. Kim, S. Mho, W. Cho and I. H. Yeo, *Electrochim. Acta*, 2010, **55**, 8023.
- 59 G. M. Suppes, B. A. Deore and M. S. Freund, *Langmuir*, 2008, **24**, 1064.
- 60 V. Egan, R. Bernstein, L. Hohmann, T. Tran and R. B. Kaner, *Chem. Commun.*, 2001, 801.
- 61 J. L. Bredas and G. B. Street, *Acc. Chem. Res.*, 1985, **18**, 309.
- 62 S. O. Vilela, M. A. Soto-Oviedo, A. P. F. Albers and R. Faez, *Mater. Res.*, 2007, **10**, 297.
- 63 H. Naarmann, *Polymers, Electrically Conducting Ullmann's*, Encyclopedia of Industrial Chemistry, 2000.
- 64 H. S. Nalwa, *Handbook of Nanostructured Materials and Nanotechnology*, ed. Academic Press, New York, NY, USA, 2000, vol. 5, p. 501.
- 65 H. Shirakawa, E. J. Lewis, A. G. MacDiarmid, C. K. Chiang and A. Heeger, *J. Chem. Soc., Chem. Commun.*, 1977, 578.
- 66 H. J. Boweley, D. L. Gerrard and W. F. Maddams, *Makromol. Chem.*, 1985, **186**, 715.
- 67 H. Shirakawa, *Angew. Chem., Int. Ed.*, 2001, **40**, 2574.
- 68 T. Ito, H. Shirakawa and I. J. Ikeda, *J. Polym. Sci., Polym. Chem. Ed.*, 1974, **12**, 11.
- 69 L. Dai, *J. Macromol. Sci., Rev. Macromol. Chem. Phys.*, 1999, **39**, 273.
- 70 G. L. Baker, in *Electronic and Photonic Applications of Polymers*, ed. M. J. Bowden and S. R. Turner, Adv. Chem. Ser. 218, ACS, Washington DC, 1988.
- 71 S. P. Armes, *Curr. Opin. Colloid Interface Sci.*, 1996, **1**, 214.
- 72 *Carbon Rich Compounds II, Macrocyclic Oligoacetylenes and Other Linearly Conjugated Systems*, ed. A. de Meijere, Springer-Verlag, Berlin, 1999.
- 73 K. Yoshino, M. Hirohata, R. Hidayat, K. Tada, T. Sada, M. Teraguchi, V. M. Frolov, S. M. Shkunov, Z. V. Vardeny and M. Hamaguchi, *Synth. Met.*, 1997, **91**, 283.

- 74 K. Tamao, S. Kodama, I. Nakajima, M. Kumada, A. Minato and S. Suzuki, *Tetrahedron*, 1982, **38**, 3347.
- 75 J. M. Tour, *Adv. Mater.*, 1994, **6**, 190.
- 76 *Conjugated Polymers*, ed. J. L. Bredas and R. Silbey, Kluwer Academic, Dordrecht, 1991.
- 77 H. Meier, M. Lehmann and U. Kolb, *Chem.–Eur. J.*, 2000, **6**, 2462.
- 78 *Handbook of Conducting Polymers*, ed. T. A. Skotheim, R. L. Elsenbaumer and J. R. Reynolds, Marcel Dekker, New York, 1998.
- 79 J. Heinze, B. Frontana, A. Uribe and S. Ludwigs, *Chem. Rev.*, 2010, **110**, 4724.
- 80 Y. Z. Long, M. M. Li, C. Gu, M. Wan, J. L. Duvail, Z. Liue and Z. Fan, *Prog. Polym. Sci.*, 2011, **36**, 1415.
- 81 J. X. Huang, S. Virji, B. H. Weiller and R. B. Kaner, *J. Am. Chem. Soc.*, 2003, **125**, 314.
- 82 J. X. Huang and R. B. Kaner, *J. Am. Chem. Soc.*, 2004, **126**, 851.
- 83 N. R. Chiou and A. J. Epstein, *Adv. Mater.*, 2005, **17**, 1679.
- 84 M. X. Wan, *Adv. Mater.*, 2008, **20**, 2926.
- 85 M. X. Wan, J. Huang and Y. Q. Shen, *Synth. Met.*, 1999, **101**, 708.
- 86 J. X. Huang and R. B. Kaner, *Angew. Chem., Int. Ed.*, 2004, **43**, 5817.
- 87 J. Jang and H. Yoon, *Chem. Commun.*, 2003, 720.
- 88 H. Liu, X. B. Hu, J. Y. Wang and R. I. Boughton, *Macromolecules*, 2002, **35**, 9414.
- 89 S. K. Pillalamarri, F. D. Blum, A. T. Tokuhira, J. G. Story and M. F. Bertino, *Chem. Mater.*, 2005, **17**, 227.
- 90 Z. M. Huang, Y. Z. Zhang, M. Kotaki and S. Ramakrishna, *Compos. Sci. Technol.*, 2003, **63**, 2223.
- 91 I. D. Norris, M. M. Shaker, F. K. Ko and A. G. MacDiarmid, *Synth. Met.*, 2000, **114**, 109.
- 92 C. Y. Huang, B. Dong, N. Lu, N. J. Yang, L. G. Gao, L. Tian, D. P. Qi, Q. Wu and L. F. Chi, *Small*, 2009, **5**, 583.
- 93 P. S. Thapa, D. J. Yu, J. P. Wicksted, J. A. Hadwiger, J. N. Barisci, R. H. Baughman and B. N. Flanders, *Appl. Phys. Lett.*, 2009, **94**, 033104.
- 94 S. Samitsu, T. Shimomura, K. Ito, M. Fujimori, S. Heike and T. Hashizume, *Appl. Phys. Lett.*, 2005, **86**, 233103.
- 95 S. Samitsu, Y. Takanishi and J. Yamamota, *Macromolecules*, 2009, **42**, 4366.
- 96 H. Shirakawa, E. J. Louis, A. G. MacDiarmid, C. K. Chiang and A. J. Heeger, *J. Chem. Soc., Chem. Commun.*, 1977, **16**, 578–580.
- 97 J. Rissler, *Chem. Phys. Lett.*, 2004, **395**, 92.
- 98 A. J. Heeger, *Angew. Chem., Int. Ed.*, 2001, **40**, 2591.
- 99 T. Michinobu, *Chem. Soc. Rev.*, 2011, **40**, 2306.
- 100 G. Wang, L. Zhang and J. Zhang, *Chem. Soc. Rev.*, 2012, **41**, 797.
- 101 N. Basescu, Z. X. Liu, D. Moses, A. J. Heeger, H. Naarmann and N. Theophilou, *Nature*, 1987, **327**, 403.
- 102 J. L. Bredas, D. Beljonne, V. Coropceanu and J. Cornil, *Chem. Rev.*, 2004, **104**, 4971.
- 103 M. Mueller, M. Fabretto, D. Evans, P. Hojati-Talemi, C. Gruber and P. Murphy, *Polymer*, 2012, **53**, 2146.
- 104 S. Bruckenstein, K. Brzezinska and A. R. Hillman, *Electrochim. Acta*, 2000, **45**, 3801.
- 105 S. I. Cho and S. B. Lee, *Acc. Chem. Res.*, 2008, **41**, 699.
- 106 M. D. Levi and D. Aurbach, *J. Power Sources*, 2008, **180**, 902.
- 107 J. W. Jeon, J. O'Neal, L. Shao and J. L. Lutkenhaus, *ACS Appl. Mater. Interfaces*, 2013, **5**, 10127.
- 108 S. W. Lee, B. M. Gallant, H. R. Byon, P. T. Hammond and Y. Shao-Horn, *Energy Environ. Sci.*, 2011, **4**, 1972.
- 109 D. A. Pasquier, A. Laforgue, P. Simon, G. G. Amatucci and J. F. Fauvarque, *J. Electrochem. Soc.*, 2002, **149**, A302.
- 110 S. Bhadra, D. Khastgir, N. K. Singha and J. H. Lee, *Prog. Polym. Sci.*, 2009, **34**, 783.
- 111 J. H. Cheung, W. B. Stockton and M. F. Rubner, *Macromolecules*, 1997, **30**, 2712.
- 112 D. Li, J. Huang and R. B. Kaner, *Acc. Chem. Res.*, 2008, **42**, 135.
- 113 I. Dumitrescu, P. R. Unwin and J. V. Macpherson, *Chem. Commun.*, 2009, 6886.
- 114 L. Wei and G. Yushin, *Nano Energy*, 2012, **1**, 552.
- 115 H. D. Tran, D. Li and R. B. Kaner, *Adv. Mater.*, 2009, **21**, 1487.
- 116 K. S. Park, S. B. Schougaard and J. B. Goodenough, *Adv. Mater.*, 2007, **19**, 848.
- 117 C. Su, Y. Ye, L. Xu and C. Zhang, *J. Mater. Chem.*, 2012, **22**, 22658.
- 118 M. Aydin, B. Esat, C. Kilic, M. E. Kose, A. Ata and F. Yilmaz, *Eur. Polym. J.*, 2011, **47**, 2283.
- 119 M. Zhou, J. Qian, X. Ai and H. Yang, *Adv. Mater.*, 2011, **23**, 4913.
- 120 R. D. McCullough and S. P. Williams, *J. Am. Chem. Soc.*, 1993, **115**, 11608.
- 121 G. Liu, S. Xun, N. Vukmirovic, X. Song, O.-P. Velasco, H. Zheng, V. S. Battaglia, L. Wang and W. Yang, *Adv. Mater.*, 2011, **23**, 4679.
- 122 C. Y. Wang, A. M. Ballantyne, S. B. Hall, C. O. Too, D. L. Officer and G. G. Wallace, *J. Power Sources*, 2006, **156**, 610.
- 123 Y. Liao, V. Strong, W. Chian, X. Wang, X. G. Li and R. B. Kaner, *Macromolecules*, 2012, **45**, 1570.
- 124 H. R. Ghenaatian, M. F. Mousavi, S. H. Kazemi and M. Shamsipur, *Synth. Met.*, 2009, **159**, 1717.
- 125 H. R. Ghenaatian, M. F. Mousavi and M. S. Rahmanifar, *Electrochim. Acta*, 2012, **78**, 212.
- 126 L. J. Bian, F. Luan, S. S. Liu and X. X. Liu, *Electrochim. Acta*, 2012, **64**, 17.
- 127 S. N. Patel, A. E. Javier, K. M. Beers, J. A. Pople, V. Ho, R. A. Segalman and N. P. Balsara, *Nano Lett.*, 2012, **12**, 4901.
- 128 S. N. Patel, A. E. Javier, G. M. Stone, S. A. Mullin and N. P. Balsara, *ACS Nano*, 2012, **6**, 1589.
- 129 Z. F. Li, H. Zhang, Q. Liu, Y. Liu, L. Stanciu and J. Xie, *ACS Appl. Mater. Interfaces*, 2014, **6**, 5996.
- 130 C. Ban, Z. Li, Z. Wu, M. J. Kirkham, L. Chen, Y. S. Jung, E. A. Payzant, Y. Yan, M. S. Whittingham and A. C. Dillon, *Adv. Energy Mater.*, 2011, **1**, 58.
- 131 J. S. Lee, S. Tai Kim, R. Cao, N. S. Choi, M. Liu, K. T. Lee and J. Cho, *Adv. Energy Mater.*, 2011, **1**, 34.

- 132 J. F. Mike and J. L. Lutkenhaus, *J. Polym. Sci., Part B: Polym. Phys.*, 2013, **51**, 468.
- 133 Z. Liu, S. Poyraz, Y. Liu and X. Zhang, *Nanoscale*, 2012, **4**, 106.
- 134 J. M. Pringle, O. Winther-Jensen, C. Lynam, G. G. Wallace, M. Forsyth and D. R. MacFarlane, *Adv. Funct. Mater.*, 2008, **18**, 2031.
- 135 X. Feng, H. Huang, Q. Ye, J. J. Zhu and W. Hou, *J. Phys. Chem. C*, 2007, **111**, 8463.
- 136 D. Munoz-Rojas, J. Oro-Sole, O. Ayyad and P. J. Gomez-Romero, *Mater. Chem.*, 2011, **21**, 2078.
- 137 Z. Liu, Y. Liu, L. Zhang, S. Poyraz, N. Lu, M. Kim, J. Smith, X. Wang, Y. Yu and X. Zhang, *Nanotechnology*, 2012, **23**, 335603.
- 138 M. K. Song, S. Park, F. M. Alamgir, J. Cho and M. Liu, *Mater. Sci. Eng., R*, 2011, **72**, 203.
- 139 F. Leroux, G. Goward, W. P. Power and L. F. Nazar, *J. Electrochem. Soc.*, 1997, **144**, 3886.
- 140 F. Huguenin, R. M. Torresi and D. A. Buttry, *J. Electrochem. Soc.*, 2002, **149**, A546.
- 141 S. L. Chou, X. W. Gao, J. Z. Wang, D. Wexler, Z. X. Wang, L. Q. Chend and H. K. Liu, *Dalton Trans.*, 2011, **40**, 12801.
- 142 S. R. Sivakkumar and D. W. Kim, *J. Electrochem. Soc.*, 2007, **154**, A134.
- 143 D. Zhang, Y. Yin, C. Liu and S. Fan, *Chem. Commun.*, 2015, **51**, 322.
- 144 W. Xiao, J. S. Chen, Q. Lu and X. W. Lou, *J. Phys. Chem. C*, 2010, **114**, 12048.
- 145 L. Yang, S. Wang, J. Mao, J. Deng, Q. Gao, Y. Tang and O. G. Schmidt, *Adv. Mater.*, 2013, **25**, 1180.
- 146 Y. G. Wang, Y. R. Wang, E. J. Hosono, K. X. Wang and H. S. Zhou, *Angew. Chem., Int. Ed.*, 2008, **47**, 7461.
- 147 Z. Ding, B. Yao, J. Feng and J. Zhang, *J. Mater. Chem. A*, 2013, **1**, 11200.
- 148 L. Yue, S. Wang, X. Zhao and L. Zhang, *J. Mater. Chem.*, 2012, **22**, 1094.
- 149 C. Arbizzani, M. Mastragostino and M. Rossi, *Electrochem. Commun.*, 2002, **4**, 545.
- 150 H. Wang, Y. Zeng, K. Huang, S. Liu and L. Chen, *Electrochim. Acta*, 2007, **52**, 5102.
- 151 Y. G. Wang, W. Wu, L. Cheng, P. He, C. X. Wang and Y. Y. Xia, *Adv. Mater.*, 2008, **20**, 2166.
- 152 L. Mai, X. Xu, C. Han, Y. Luo, L. Xu, Y. A. Wu and Y. Zhao, *Nano Lett.*, 2011, **11**, 4992.
- 153 I. Boyano, M. Bengoechea, I. de Meatza, O. Miguel, I. Cantero, E. Ochoteco, J. Rodriguez, M. L. Cantu and P. G. Romero, *J. Power Sources*, 2007, **166**, 471.
- 154 Z. P. Guo, J. Z. Wang, H. K. Liu and S. X. Dou, *J. Power Sources*, 2005, **146**, 448.
- 155 X. Y. Zhou, J. Tang, J. Yang, Y. L. Zou, S. C. Wang, J. Xie and L. L. Ma, *Electrochim. Acta*, 2012, **70**, 296.
- 156 C. X. Guo, M. Wang, T. Chen, X. W. Lou and C. M. Li, *Adv. Energy Mater.*, 2011, **1**, 736.
- 157 Y. Chen, S. Zeng, J. Qian, Y. Wang, Y. Cao, H. Yang and X. Ai, *ACS Appl. Mater. Interfaces*, 2014, **6**, 3508.
- 158 M. V. Reddy, B. L. W. Wen, K. P. Loh and B. V. R. Chowdari, *ACS Appl. Mater. Interfaces*, 2013, **5**, 7777.
- 159 Z. P. Guo, J. Z. Wang, H. K. Liu and S. X. Dou, *J. Power Sources*, 2005, **146**, 448.
- 160 S. Kuwabata, S. Masui and H. Yoneyama, *Electrochim. Acta*, 1999, **44**, 4593.
- 161 J. K. Kim, J. Manuel, M. H. Lee, J. Scheers, D. H. Lim, P. Johansson, J. H. Ahn, A. Matic and P. Jacobsson, *J. Mater. Chem.*, 2012, **22**, 15045.
- 162 Y. H. Wang, H. Liu, D. Zhu, Z. P. Guo, H.-K. Liu and S. X. Dou, *Trans. Nonferrous Met. Soc. China*, 2011, **21**, 1303.
- 163 H. Zhao, A. Yuan, B. Liu, S. Xing, X. Wu and J. Xu, *J. Appl. Electrochem.*, 2012, **42**, 139.
- 164 I. Boyano, M. Bengoechea, I. de Meatza, O. Miguel, I. Cantero, E. Ochoteco, J. Rodriguez, M. Lira-Cantu and P. Gomez-Romero, *J. Power Sources*, 2007, **166**, 471.
- 165 O. Y. Posudievsky, O. A. Kozarenko, V. S. Dyadyun, S. W. Jorgensen, J. A. Spearot, V. G. Koshechko and V. D. Pokhodenko, *Electrochim. Acta*, 2011, **58**, 442.
- 166 H. C. Dinh, S. I. Mho and I. H. Yeo, *Electroanalysis*, 2011, **23**, 2079–2086.
- 167 A. H. Gemeay, H. Nishiyama, S. Kuwabata and H. Yoneyama, *J. Electrochem. Soc.*, 1995, **142**, 4190.
- 168 S. Kuwabata, S. Masui and H. Yoneyama, *Electrochim. Acta*, 1999, **44**, 4593.
- 169 I. Boyano, M. Bengoechea, I. de Meatza, O. Miguel, I. Cantero, E. Ochoteco, H. Grande, M. L. Cantu and P. G. Romero, *J. Power Sources*, 2007, **174**, 1206.
- 170 X. Xia, Z. Wang and L. Chen, *Electrochem. Commun.*, 2008, **10**, 1442.
- 171 D. Lepage, C. Michot, G. Liang, N. Gauthier and S. B. Schougaard, *Angew. Chem., Int. Ed.*, 2011, **50**, 6884.
- 172 H. Wu, G. Yu, L. Pan, N. Liu, M. T. McDowell, Z. Bao and Y. Cui, *Nat. Commun.*, 2013, **4**, 1943.
- 173 B. Liu, P. Soares, C. Checkles, Y. Zhao and G. Yu, *Nano Lett.*, 2013, **13**, 3414.
- 174 L. J. Fu, H. Liu, C. Li, Y. P. Wu, E. Rahm, R. Holze and H. Q. Wu, *Prog. Mater. Sci.*, 2005, **50**, 881.
- 175 X. Ren, C. Shi, P. Zhang, Y. Jiang, J. Liu and Q. Zhang, *Mater. Sci. Eng., B*, 2012, **177**, 929.
- 176 F. Huguenin, E. M. Giroto, R. M. Torresi and D. A. Buttry, *J. Electroanal. Chem.*, 2002, **536**, 37.
- 177 F. Huguenin, E. A. Ticianelli and R. M. Torresi, *Electrochim. Acta*, 2002, **47**, 3179.
- 178 M. L. Cantu and P. G. Romero, *J. Solid State Chem.*, 1999, **147**, 601.
- 179 M. L. Cantu and P. G. Romero, *J. Electrochem. Soc.*, 1999, **146**, 2029.
- 180 M. G. Kanatzidis, C. R. Kannewurf, H. O. Marcy and C. G. Wu, *J. Am. Chem. Soc.*, 1989, **111**, 4139.
- 181 K. I. Park, H. M. Song, Y. Kim, S. I. Mho, W. I. Cho and I. H. Yeo, *Electrochim. Acta*, 2010, **55**, 8023.
- 182 H. Ze-qiang, X. Li-zhi, C. Shang, W. Xian-ming, L. Wen-ping and H. Ke-long, *Trans. Nonferrous Met. Soc. China*, 2010, **20**, s262.
- 183 Y. H. Huang, K. S. Park and J. B. Goodenough, *J. Electrochem. Soc.*, 2006, **153**, A2282.
- 184 A. V. Murugan, *Electrochim. Acta*, 2005, **50**, 4627.



- 185 Q. Gong, Y. S. He, Y. Yang, X. Z. Liao and Z. F. Ma, *J. Solid State Electrochem.*, 2012, **16**, 1383.
- 186 Z. Du, S. Zhang, Y. Liu, J. Zhao, R. Lin and T. Jiang, *J. Mater. Chem.*, 2012, **22**, 11636.
- 187 J. B. Bates, N. J. Dudney, D. C. Lubben, G. R. Gruzalski, B. S. Kwak, X. Yu and R. A. Zuhr, *J. Power Sources*, 1995, **54**, 58.
- 188 N. J. Dudney, *J. Electrochem. Soc. Interface*, 2008, **3**, 44.
- 189 S. W. Song, H. Choi, H. Y. Park, G. B. Park, K. C. Lee and H. J. Lee, *J. Power Sources*, 2010, **195**, 8275.
- 190 J. Z. Wang, S. L. Chou, J. Chen, S. Y. Chew, G. X. Wang, K. Konstantinov, J. Wu, S. X. Dou and H. K. Liu, *Electrochem. Commun.*, 2008, **10**, 1781.
- 191 X. H. Huang, J. P. Tu, X. H. Xia, X. L. Wang and J. Y. Xiang, *Electrochem. Commun.*, 2008, **10**, 1288.
- 192 X. H. Huang, J. P. Tu, X. H. Xia, X. L. Wang, J. Y. Xiang and L. Zhang, *J. Power Sources*, 2010, **195**, 1207.
- 193 J. Z. Wang, S. L. Chou, J. Chen, S. Y. Chew, G. X. Wang, K. Konstantinov, J. Wu, S. X. Dou and H. K. Liu, *Electrochem. Commun.*, 2008, **10**, 1781.
- 194 G. X. Wang, L. Yang, Y. Chen, J. Z. Wang, S. Bewlay and H. K. Liu, *Electrochim. Acta*, 2005, **50**, 4649.
- 195 Y. H. Huang, K. S. Park and J. B. Goodenough, *J. Electrochem. Soc.*, 2006, **153**, A2282.
- 196 X. Y. Zhou, J. J. Tang, J. Yang, Y. L. Zou, S. C. Wang, J. Xie and L. L. Ma, *Electrochim. Acta*, 2012, **70**, 296.
- 197 Y. Yao, N. Liu, M. T. McDowell, M. Pasta and Y. Cui, *Energy Environ. Sci.*, 2012, **5**, 7927.
- 198 Y. Wang, Y. Wang, J. Tang, Y. Xia and G. Zheng, *J. Mater. Chem. A*, 2014, **2**, 20177.
- 199 D. Kundu, F. Krumeich and R. Nesper, *J. Power Sources*, 2013, **236**, 112.
- 200 L. Shao, J. W. Jeon and J. L. Lutkenhaus, *Chem. Mater.*, 2012, **24**, 181.
- 201 W. M. Chen, Y. H. Huang and L. X. Yuan, *J. Electroanal. Chem.*, 2011, **660**, 108.
- 202 N. H. Idris, J. Wang, S. Chou, C. Zhong, M. M. Rahman and H. Liu, *J. Mater. Res.*, 2011, **26**, 860.
- 203 G. J. Wang, L. C. Yang, Q. T. Qu, B. Wang, Y. P. Wu and R. Holze, *J. Solid State Electrochem.*, 2010, **14**, 865.
- 204 W. Tang, L. Liu, Y. Zhu, H. Sun, Y. Wu and K. Zhu, *Energy Environ. Sci.*, 2012, **5**, 6909.
- 205 W. Tang, X. W. Gao, Y. S. Zhu, Y. B. Yue, Y. Shi, Y. P. Wu and K. Zhu, *J. Mater. Chem.*, 2012, **22**, 20143.
- 206 L. L. Liu, X. J. Wang, Y. S. Zhu, C. L. Hu, Y. P. Wu and R. Holze, *J. Power Sources*, 2013, **224**, 290.
- 207 F. Tian, L. Liu, Z. Yang, X. Wang, Q. Chen and X. Wang, *Mater. Chem. Phys.*, 2011, **127**, 151.
- 208 A. E. Javier, S. N. Patel, D. T. Hallinan Jr, V. Srinivasan and N. P. Balsara, *Angew. Chem., Int. Ed.*, 2011, **50**, 9848.
- 209 Z. J. Zhang, J. Z. Wang, S. L. Chou, H. K. Liu, K. Ozawa and H. J. Li, *Electrochim. Acta*, 2013, **108**, 820.
- 210 Y. Chen, S. Zeng, J. Qian, Y. Wang, Y. Cao, H. Yang and X. Ai, *ACS Appl. Mater. Interfaces*, 2014, **6**, 3508.
- 211 F. Han, D. Li, W. C. Li, C. Lei, Q. Sun and A. H. Lu, *Adv. Funct. Mater.*, 2013, **23**, 1692.
- 212 L. Cui, J. Shen, F. Cheng, Z. Tao and J. Chen, *J. Power Sources*, 2011, **196**, 2195.
- 213 L. Yuan, J. Wang, S. Y. Chew, J. Chen, Z. P. Guo, L. Zhao, K. Konstantinov and H. K. Liu, *J. Power Sources*, 2007, **174**, 1183.
- 214 S. Y. Chew, Z. P. Guo, J. Z. Wang, J. Chen, P. Munroe, S. H. Ng, L. Zhao and H. K. Liu, *Electrochem. Commun.*, 2007, **9**, 941.
- 215 Z. Q. He, L. Z. Xiong, W. P. Liu, X. M. Wu, S. Chen and K. L. Huang, *J. Cent. South Univ. Technol.*, 2008, **15**, 214.
- 216 Q. G. Shao, W. M. Chen, Z. H. Wang, L. Qie, L. X. Yuan, W. X. Zhang, X. L. Hu and Y. H. Huang, *Electrochem. Commun.*, 2011, **13**, 1431.
- 217 R. Liang, H. Cao, D. Qian, J. Zhang and M. Qu, *J. Mater. Chem.*, 2011, **21**, 17654.
- 218 Y. Zhao, J. Li, N. Wang, C. Wu, G. Dong and L. Guan, *J. Phys. Chem. C*, 2012, **116**, 18612.
- 219 C. Lai, H. Z. Zhang, G. R. Li and X. P. Gao, *J. Power Sources*, 2011, **196**, 4735.
- 220 C. Lai, G. R. Li, Y. Y. Dou and X. P. Gao, *Electrochim. Acta*, 2010, **55**, 4567.
- 221 F. Zhang, H. Cao, D. Yue, J. Zhang and M. Qu, *Inorg. Chem.*, 2012, **51**, 9544.
- 222 Z. Yin, Y. Ding, Q. Zheng and L. Guan, *Electrochem. Commun.*, 2012, **20**, 40.
- 223 R. Vidu and P. Stroeve, *Ind. Eng. Chem. Res.*, 2004, **43**, 3314.
- 224 N. H. Idris, J. Wang, S. Chou, C. Zhong, M. M. Rahman and H. Liu, *J. Mater. Res.*, 2011, **26**, 860.
- 225 C. J. Cui, G. M. Wu, H. Y. Yang, S. F. She, J. Shen, B. Zhou and Z. H. Zhang, *Electrochim. Acta*, 2010, **55**, 8870.
- 226 H. Wang, K. Huang, Y. Zeng, F. Zhao and L. Chen, *Electrochem. Solid-State Lett.*, 2007, **10**, A199.
- 227 A. Fedorkova, A. N. Alejos, P. G. Romero, R. Orinakovac and D. Kaniansky, *Electrochim. Acta*, 2010, **55**, 943.
- 228 Y. Fu and A. Manthiram, *Chem. Mater.*, 2012, **24**, 3081.
- 229 J. J. Cai, P. J. Zuo, X. Q. Cheng, Y. H. Xu and G. P. Yin, *Electrochem. Commun.*, 2010, **12**, 1572.
- 230 E. A. Ponzio, T. M. Benedetti and R. M. Torresi, *Electrochim. Acta*, 2007, **52**, 4419.
- 231 K. S. Hwang, C. W. Lee, T. H. Yoon and Y. S. Son, *J. Power Sources*, 1999, **79**, 225.
- 232 T. A. Kerr, H. Wu and L. F. Nazar, *Chem. Mater.*, 1996, **8**, 2005.
- 233 G. T. Gomez, E. M. T. Rosales and P. G. Romero, *Chem. Mater.*, 2001, **13**, 3693.
- 234 X. W. Zhang, C. Wang, A. J. Appleby and F. E. Little, *J. Power Sources*, 2002, **109**, 136.
- 235 G. Liu, S. Xun, N. Vukmirovic, X. Song, P. O. Velasco, H. Zheng, V. S. Battaglia, L. Wang and W. Yang, *Adv. Mater.*, 2011, **23**, 4679.
- 236 S. Xun, X. Song, V. Battaglia and G. Liu, *J. Electrochem. Soc.*, 2013, **160**, A849.
- 237 M. Gu, X. C. Xiao, G. Liu, S. Thevuthasan, D. R. Baer, J. G. Zhang, J. Liu, N. D. Browning and C. M. Wang, *Sci. Rep.*, 2014, **4**, 3684.
- 238 M. Wu, X. Xiao, N. Vukmirovic, S. Xun, P. K. Das, X. Song, P. O. Velasco, D. Wang, A. Z. Weber, L. W. Wang,

- V. S. Battaglia, W. Yang and G. Liu, *J. Am. Chem. Soc.*, 2013, **135**, 12048.
- 239 D. Chao, X. Xia, J. Liu, Z. Fan, C. F. Ng, J. Lin, H. Zhang, Z. X. Shen and H. J. Fan, *Adv. Mater.*, 2014, **26**, 5794.
- 240 S. Wang, L. Hu, Y. Hu and S. Jiao, *Mater. Chem. Phys.*, 2014, **146**, 289.
- 241 F. Wu, J. Chen, L. Li, T. Zhao, Z. Liu and R. Chen, *ChemSusChem*, 2013, **6**, 1438.
- 242 Y. H. Huang and J. B. Goodenough, *Chem. Mater.*, 2008, **20**, 7237.
- 243 Z. Chen, J. W. F. To, C. Wang, Z. Lu, N. Liu, A. Chortos, L. Pan, F. Wei, Y. Cui and Z. Bao, *Adv. Energy Mater.*, 2014, **4**, 1400207.
- 244 G. Ma, Z. Wen, J. Jin, Y. Lu, X. Wu, C. Liu and C. Chen, *RSC Adv.*, 2014, **4**, 21612.
- 245 M. Pasta, C. D. Wessells, R. A. Huggins and Y. Cui, *Nat. Commun.*, 2012, **1149**, 3.
- 246 Z. W. Seh, H. Wang, P. Hsu, Q. Zhang, W. Li, G. Zheng, H. Yao and Y. Cui, *Energy Environ. Sci.*, 2014, **7**, 672.
- 247 H. Chen, W. Dong, J. Ge, C. Wang, X. Wu, W. Lu and L. Chen, *Sci. Rep.*, 2013, **3**, 1910.